

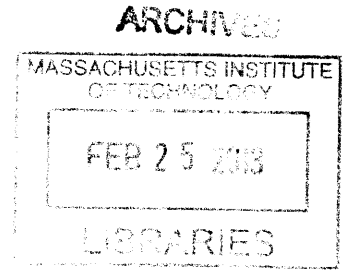
Intracranial Electroencephalography Signatures of the Induction of
General Anesthesia with Propofol

by

Veronica Sara Weiner

M.A. Artificial Intelligence, Modeling, and Formalization
University of Paris VI, 2003

B.S. Brain and Cognitive Sciences, B.S. Economics, B.S. Management
Massachusetts Institute of Technology, 2001, 2001, 2002



SUBMITTED TO THE DEPARTMENT OF BRAIN AND COGNITIVE SCIENCES IN PARTIAL
FULLFILLMENT OF THE REQUIREMENTS FOR THE DEGREE OF
DOCTOR OF PHILOSOPHY IN BRAIN AND COGNITIVE SCIENCE
AT THE
MASSACHUSETTS INSTITUTE OF TECHNOLOGY

FEBRUARY 2013

©2013 Veronica Weiner. All rights reserved.
The author hereby grants to MIT permission to reproduce
and to distribute publicly paper and electronic
copies of this thesis document in whole or in part
in any medium now known or hereafter created.

Signature of author: _____

Department of Brain and Cognitive Sciences
January 11, 2013

Certified by: _____

Emery N. Brown, M.D., Ph.D.
Professor of Brain and Cognitive Sciences
Thesis Co-supervisor

Certified by: _____

Patrick L. Purdon, Ph.D.
Instructor of Anaesthesia at Harvard Medical School
Thesis Co-supervisor

Accepted by: _____

Matthew Wilson, Ph.D.
Professor of Brain and Cognitive Sciences
Chairman, Committee for Graduate Students

Intracranial Electroencephalography Signatures of the Induction of General Anesthesia with Propofol

by
Veronica Sara Weiner

Submitted to the MIT Department of Brain and Cognitive Sciences in partial fulfillment of the requirements for the degree of Doctor of Philosophy in Neuroscience on January 6, 2013

Abstract

General anesthesia is a drug-induced, reversible behavioral state characterized by hypnosis (loss of consciousness), amnesia (loss of memory), analgesia (loss of pain perception), akinesia (loss of movement), and hemodynamic stability (stability and control of the cardiovascular, respiratory, and autonomic nervous systems). Each year, more than 25 million patients receive general anesthesia in the United States. Anesthesia-related morbidity is a significant medical problem, including nausea, vomiting, respiratory distress, post-operative cognitive dysfunction, and post-operative recall. To eliminate anesthesia-related morbidity, the brain systems involved in producing general anesthesia must be identified and characterized, and methods must be devised to monitor those brain systems and guide drug administration. A priority for anesthesia research is to identify the brain networks responsible for the characteristic electroencephalography (EEG) signals of anesthesia in relation to sensory, cognitive, memory, and pain systems.

In this thesis, we recorded simultaneous intracranial and surface EEG, and single unit data in patients with intractable epilepsy who had been previously implanted with clinical and/or research electrodes. The aims of this research were to characterize the neural signals of anesthesia in a regionally and temporally precise way that is relevant to clinical anesthesia, and to identify dynamic neuronal networks that underlie these signals. We demonstrated region-specific, frequency-band-specific changes in neural recordings at loss of consciousness. We related these findings to theories of how anesthetic drugs may impart their behavioral effects.

Thesis supervisors: Patrick L. Purdon, Ph.D.
Instructor of Anaesthesia
Harvard Medical School

Emery N. Brown, M.D., Ph.D.
Professor of Computational Neuroscience and Health Sciences and Technology
MIT Department of Brain and Cognitive Sciences
MIT-Harvard Division of Health Sciences and Technology

Biographical Note

Veronica S. Weiner
908.907.1419
vsw@alum.mit.edu

Education

Massachusetts Institute of Technology Cambridge, MA
Doctor of Philosophy Expected: February 2013
Neuroscience
Thesis supervisors: Patrick L. Purdon and Emery N. Brown
Thesis committee chair: Matt A. Wilson

Ecole Polytechnique, Ecole Normale Supérieure, Univ. Paris VI (joint program) Paris, France
Master of Science July 2003
Artificial Intelligence, Modeling, and Formalization
Supervisor: Alain Berthoz

Massachusetts Institute of Technology Cambridge, MA
Bachelor of Science June 2002
Brain and Cognitive Sciences – computation option
Economics
Management

Ecole Polytechnique Palaiseau, France
Visiting student January-May 2002
Economics

Awards

Singleton Graduate Fellowship (2010)
Massachusetts General Hospital, Department of Anesthesia Clinical Research Day award for student research (2010)
National Science Foundation Graduate Fellowship
Sigma Xi, Scientific Honor Society (2002)

Publications

Mukamel EA, Pirodini E, Babadi B, Wong KFK, Pierce ET, Harrell G, Walsh JL, Salazar-Gomez AF, Cash S, Eskandar E, Weiner VS, Brown EN, Purdon PL. A novel transition in brain state during general anesthesia. Manuscript in submission.

Lewis LD, Ching S, Weiner VS, Peterfreund RA, Eskandar EN, Cash SS, Brown EN, Purdon PL. Local cortical dynamics of burst suppression in the anesthetized brain. Manuscript in submission.

Lewis LD, Weiner VS, Mukamel EA, Donoghue JA, Eskandar EN, Madsen JR, Anderson WS, Hochberg LR, Cash SS, Brown EN, Purdon PL.(2012) Rapid fragmentation of neuronal networks at the onset of

propofol-induced unconsciousness. *Proc Natl Acad Sci.* 109 (49).

Schiller PH, Slocum WM, Jao B, Weiner VS. (2011) The integration of disparity, shading and motion parallax cues for depth perception in humans and monkeys. *Brain Research.*

Chen Z, Weiner VS, Ching S, Putrino DF, Cash S, Kopell N, Purdon PL, & Brown EN. (2010) Assessing neuronal interactions of assemblies during general anesthesia. *IEEE Engineering in Medicine and Biology Conference, Buenos Aires, Argentina.*

Zhang Y, Weiner VS, Slocum WM & Schiller PH. (2007) Depth from shading and disparity in humans and monkeys. *Visual Neuroscience.* 24, 207-215.

Schiller PH, Slocum WM, & VS Weiner. (2007) How the parallel channels of the retina contribute to depth processing. *European Journal of Neuroscience.* 26 (5), 1307-1321.

Conference abstracts

Weiner VS, Cash SS, Eskandar EN, Peterfreund RA, Pierce ET, Szabo MD, Salazar AF, Chan AM, Cormier JE, Dykstra AR, Zepeda R, Brown EN, & Purdon PL (2010). Coherent activity in brain areas subserving memory function after induction of propofol anesthesia. *Society for Neuroscience Meeting.*

Weiner VS, Cash SS, Eskandar EN, Peterfreund RA, Pierce ET, Szabo MD, Salazar AF, Chan AM, Cormier JE, Dykstra AR, Zepeda R, Brown EN, & Purdon PL (2009). Intracranial neural recordings in deep structures of the human brain during general anesthesia: implications for improved anesthetic monitoring. *Massachusetts General Hospital Clinical Research Day.*

Weiner VS & Schiller, PH (2007) The integration of disparity, shading and parallax cues for depth perception in humans and monkeys. *Society for Neuroscience Meeting.*

Weiner VS & Schiller, PH (2007) What role do the parallel channels of the retina play in the processing of stereopsis and motion parallax? *Vision Sciences Society Meeting.*

Schiller PH, Tehovnik EJ, Weiner VS (2006) Preliminary studies examining the feasibility of a visual prosthetic device: 2. The laminar specificity of electrical stimulation in monkey area V1 and the visual percepts created. *Vision Sciences Society Meeting.*

Weiner VS, Schiller PH, & Y Zhang (2006) How effective are disparity and motion parallax cues for depth perception in humans and monkeys? *Vision Sciences Society Meeting.*

Zhang Y, Schiller PH, Weiner VS, & WM Slocum (2005) Depth from shading and disparity in humans and monkeys. *Vision Sciences Society Meeting.*

Schiller PH, Weiner VS, Tehovnik EJ (2005) Preliminary studies examining the feasibility of a visual prosthetic device: 1. What does a monkey see when area V1 is stimulated electrically? *Society for*

Neuroscience Meeting.

Weiner VS, Zhang Y, and PH Schiller (2004) Interactive visual processing of stereopsis and motion parallax. Society for Neuroscience Meeting.

Talks

The action selection problem. Bayesian Inspired Brain and Artifacts Conference, France, 2003.

Service and Work Experience

MIT IDEAS Competition: Lead student organizer for MIT's social entrepreneurship and community service competition (2007-2009)

MIT McCormick Dormitory - Graduate resident tutor (2009-2012)

MIT Women's Technology program - Residential director (2008)

MIT Splash Program – Volunteer instructor in visual neuroscience (2005-2007)

MIT Student House – President (2002)

Teaching

Harvard University Neurobiology of Behavior (Sanes and Lichtman), 3 years, 7 sections

MIT Statistics (Brown)

MIT Brain Science Laboratory (Jhaveri)

MIT Core Neuroscience (Moore)

MIT Instructor in Linux and Mathematical Software, 4 years until 2002, 100+ classes

Other Research and Work experience

Mascoma, Inc. – extern, 2009, via MIT's Entrepreneurship Lab

MIT Schiller Lab - technician, 2003-2006 (Peter Schiller)

MIT Graybiel Lab – technician, 2004 (Mark Ruffo)

MIT Center for Biological and Computational Learning – UROP, 2001-2003 (Sayan Mukerjee), rotation student, 2005 (Tony Ezzat)

French National Institute for Statistics and Economics Research – analyst, 2002 (Jacques Mairesse)

MIT Department of Economics – UROP, 1997-2002 (Nancy Rose, Peter Temin)

Diogenes software – intern, 2000, B2B software company

Neomorphic software – intern, 1998, bioinformatics software company

Acknowledgements

First, I would like to express my deepest gratitude to Patrick Purdon, my research supervisor, who has been extremely patient, knowledgeable and supportive in overseeing this project. I am also very grateful to Emery Brown, who has supported me in the NeuroStat lab at MIT and guided the research to a completed thesis. I am grateful to Matt Wilson, the chair of my thesis committee, for overseeing our project milestones and for many helpful discussions. Syd Cash and Chris Moore have participated in the project as advisory members of the thesis committee and I am thankful for their knowledgeable suggestions.

I am grateful to the patients at MGH and BWH who participated in the experiments of this thesis during what must have been a challenging period of their clinical treatment.

This work is possible because of the support of many collaborators at MIT and MGH, including NeuroStat and Purdon Lab members Andres Salazar, Eran Mukamel, Michael Prerau, Aaron Sampson, Rob Haslinger, Sage Chen, Iahn Cajigas, Kevin Wong, Francisco Flores, Demba Ba, Laura Lewis, ShiNung Ching, Sheri Leone and Julie Scott, Cashlab members Alex Chan, Andy Dykstra, Rodrigo Zepeda, Justine Cormier, and Corey Keller, MGH staff Emad Eskandar, Eric Pierce, Robert Peterfreund, Michelle Szabo, and Kristi Tripp, and at MGH Charlestown the computer helpdesk and operational staff.

I am grateful to Peter Schiller for his generous and educational mentorship which led me to apply to graduate school at MIT.

Finally, I'd like to thank my family, my best friends, and especially my sister Angelica, who has given me support, love, and encouragement over many years.

Contents

Abstract	2
Biographical Note	3
Acknowledgements.....	7
List of Abbreviations	10
List of Figures and Tables.....	11
Chapter 1: Introduction	13
What is General Anesthesia?.....	13
Molecular Mechanisms of Anesthesia	14
Cellular Mechanisms of Anesthesia	15
Systems-level Mechanisms of Anesthesia	16
Staging of Anesthetic Depth using EEG.....	18
Clinical Monitoring of Anesthetic Depth.....	20
Relationship with Sleep, Coma, and Epilepsy	21
Aims of the thesis.....	21
References	23
Chapter 2: Intracranial correlates of anteriorization during propofol general anesthesia.....	27
Abstract	27
Introduction	27
Materials and Methods.....	31
Results	36
Discussion	44
References	49
Supplementary Figures.....	51
Chapter 3: Global coherence analysis of intracranial recordings during induction of propofol general anesthesia	65
Abstract	65
Introduction	66
Materials and methods	69
Results	74

Discussion	82
References	86
Supplementary Figures.....	88

List of Abbreviations

BOLD – Blood Oxygen Level Dependent

BWH – Brigham and Women’s Hospital

CT – Computerized tomography

ECoG – Electrocorticography

EEG – Electroencephalography

ERSP – Event-related spectral perturbation

fMRI – Functional magnetic resonance imaging

GA – General anesthesia

GABA - gamma-Aminobutyric acid

iEEG – Intracranial electroencephalography or intracranial electroencephalography

LOC – Loss of consciousness

MGH – Massachusetts General Hospital

MIT – Massachusetts Institute of Technology

MNI – Montreal Neurological Institute

MRI – Magnetic resonance imaging

NIH – National Institute of Health

PET – Positron emission tomography

RAS – Right, Anterior, Superior, a coordinate system in the Freesurfer software program

List of Figures and Tables

Chapter 1

Figure 1. Stages of anesthesia EEG

Chapter 2

Figure 1. Types of intracranial electrodes.

Table 1. Patient clinical and demographic information.

Figure 2. Exemplar spectrograms, Patient 9.

Figure 3. Exemplar spectrograms, Patient 3.

Figure 4. Region specific alpha power change across LOC.

Figure 5. Differences in cross frequency coupling and suppression alpha power for frontal and hippocampal channels.

Figure 6. Disruption of functional alpha rhythms at LOC.

Figure S1. Electrode coverage for all patients.

Figures S2-S12. Exemplar spectrograms for Patients 1-2, 4-8, 10-12.

Chapter 3

Figure 1. Median global coherence over patients, intracranial recordings.

Figure 2. Global coherence for each patient.

Figure 3. Mean normalized modal projection for dominant mode in the alpha band, before and after LOC.

Figure 4. Alpha band oscillatory modes before and after LOC, exemplar patients.

Figure 5. Theta band oscillatory mode before LOC, exemplar patient.

Figure 6. Delta band oscillatory mode after LOC, exemplar patient.

Figure S1. 75th percentile of spectral power, all patients.

Figure S2. Mean global coherence by frequency before LOC.

Figure S3. Mean global coherence by frequency after LOC.

Figure S4. Global coherence in all patients computed 0-40Hz.

Figure S5. Median global coherence in all patients computed 0-40Hz.

Chapter 1: Introduction

What is General Anesthesia?

General anesthesia is a drug-induced, reversible behavioral state characterized by hypnosis (loss of consciousness), amnesia (loss of memory), analgesia (loss of pain perception), akinesia (loss of movement), and hemodynamic stability (stability and control of the cardiovascular, respiratory, and autonomic nervous systems). Each year, more than 25 million patients receive general anesthesia in the United States. The systems- and network-level mechanisms of general anesthesia are a subject of current scientific investigation. Anesthesia-related morbidity is a significant medical problem: approximately 1 in 500 patients experience postoperative recall (POR) of events during surgery, up to 41% of elderly patients experience post-operative cognitive dysfunction (POCD), with long-term deficits found in 13% of such patients. Patients also frequently experience cardiorespiratory depression, perioperative nausea, and perioperative vomiting. To eliminate anesthesia-related morbidity, the brain systems involved in producing general anesthesia must be identified and characterized, and methods must be devised to monitor those brain systems and guide drug administration. Beyond the clinical importance of anesthesia research, general anesthesia provides an opportunity to study neural activity associated with conscious and unconscious states and advance scientific knowledge of neural processing.

Clinically, the state of general anesthesia is achieved using a combination of drugs that each have different effects in ensuring hypnosis, amnesia, analgesia, and akinesia during the perioperative and operative period. These include anesthetic premedications (e.g., opioids such as fentanyl and benzodiazepines such as midazolam), induction agents (e.g., propofol, sodium thiopental, etomidate, ketamine, and sevoflurane), maintenance agents (e.g., nitrous oxide, propofol, and the volatile general anesthetics), analgesics (opioids such as fentanyl), muscle

relaxants (e.g., succinylcholine, pancuronium), and other medications to treat side effects or prevent complications (e.g., antihypertensives, antibiotics). Post-operatively, medications may be given to reverse the state of general anesthesia (e.g., anticholinesterases to reverse muscle relaxation).

Molecular Mechanisms of Anesthesia

The molecular mechanisms of general anesthesia – in particular, the effects of induction and maintenance agents – have been controversial for the past century. In 1899, Meyer and Overton discovered that anesthetic potency scaled with the lipid solubility of the anesthetic agent (Dilger, 2001). This result drove the early hypothesis that anesthetic agents act within lipid bilayers of neuronal membranes. Meyer and Overton's result relating potency and lipid solubility has since been confirmed over four orders of magnitude of lipid solubility for diverse inhaled anesthetic agents including halothane, argon, xenon, nitrogen, and nitrous oxide.

In the 1990's, this early theory of anesthesia's mechanism was revised following of two discoveries: first, that volatile anesthetics are stereo-selective (Skolnick and Moody, 2001), and second, that the physical changes in lipid bilayers caused by volatile anesthetics can be mimicked by a 1 degree Celsius temperature change (Franks and Lieb, 1994). These two results suggested that the molecular mechanism of general anesthesia has more structural specificity than the mere presence an anesthetic agent within the lipid bilayer.

It is now known that anesthetic drugs act on a wide range of molecular targets in the neuronal membrane, despite causing similar changes in brain activity as measured by electroencephalogram (EEG). These molecular targets include GABA ion channels, presynaptic glutamate release mechanisms, and nicotinic acetylcholine channels Evidence for anesthetic

action at various receptor sites has been obtained from radioligand labeling studies and recombinant genetic studies specific for receptor subunits, e.g., GABA_A (Moody and Skolnick, 2001). This receptor-specific molecular mechanism can be reconciled with Meyer and Overton's early results by considering that an anesthetic agent's polarity, rather than its lipid solubility, predicts potency (Dilger, 2001).

Cellular Mechanisms of Anesthesia

Various general anesthetics have been shown to intervene at cellular level by all of the following methods: 1) enhancing the activity of inhibitory neurons, 2) reducing the activity of excitatory neurons, 3) reducing neurotransmitter release from the presynaptic cell, and 4) interfering with the generation or propagation of action potentials.

Numerous anesthetic agents have been shown to act at the GABA_A receptor, altering the time course, but not amplitude, of inhibitory currents. The mechanisms for this effect include slowing receptor deactivation and desensitization (with propofol), stabilizing the "pre-open" receptor state (also with propofol), and increasing the duration of inhibitory post-synaptic currents (with the volatile agents) (Antkowiak, 1999). The effect of the volatile agents has been shown to be dose-dependent, potentiating GABA-evoked currents at low concentrations (e.g., 3 uM) while decreasing GABA-evoked currents at high concentrations (e.g., 30-300 uM) (Antkowiak, 1999). Effects of the volatile agents on GABA-evoked currents are not well understood; enflurane and sevoflurane can actually block GABA_A activity at clinical dosages (Pearce, 2001).

In *in-vitro* cortical preparations, numerous anesthetic agents reduce the mean firing rate of neurons, and there is evidence that this effect is mediated by GABA_A receptors. Reduction in

firing rate is blocked *in-vitro* by bicuculline; *in-vivo*, anesthetic dosage requirements to achieve loss of consciousness are increased when bicuculline or picrotoxin are delivered. The specific reduction in neuronal firing rate, with respect to burst rate and intra-burst frequency, varies by anesthetic agent, suggesting that the various agents act on GABA_A receptors in different ways (Antkowiak, 1999).

Anesthetic agents may also have an effect on excitatory neurons: glutamate antagonists increase the potency of volatile agents in rats. However, it is likely that the principle mechanism of most volatile and injected agents is not glutamatergic. The known NMDA receptor antagonist ketamine produces a “dissociative” anesthetic state that is qualitatively different from the state produced by almost all other volatile and inhaled anesthetic agents. Volatile agents have also been shown to reduce excitatory currents at nicotinic ACh channels (Pearce, 2001).

Besides affecting inhibitory and excitatory currents post-synaptically, the volatile agents halothane, isoflurane, and enflurane have been shown to reduce calcium-mediated glutamate release from the nerve terminal by reducing the activity of Plasma Membrane Ca²⁺-ATPase (PMCA) in a dose-dependent manner (Hemmings, 2001). Volatile agents have also been shown to produce Na⁺ current blockage by way of inactivation hyperpolarization shifts in the sodium channel. It is controversial whether such a Na⁺ current blockage affects the propagation of action potentials or acts mainly in the pre-synaptic terminals, dendrites, somas, and initial segments of the neuron; most evidence suggests the latter.

Systems-level Mechanisms of Anesthesia

Currently, the mechanism by which cellular changes during general anesthesia induce the behavioral states of hypnosis, amnesia, and akinesia are not fully understood. The mechanisms of akinesia at the level of the spinal cord and neuromuscular junction, induced by muscle relaxants,

have been more thoroughly described, as have the mechanisms of analgesia induced by the opioids delivered in the clinical setting. (Egar et al., 1965; Prys-Roberts, 1987; Woodbridge, 1957).

Both propofol and the volatile anesthetics have been shown to globally reduce glucose metabolism and cerebral blood flow as measured in positron emission tomography (PET). In these studies, dramatic reduction has been observed across the whole brain with small regional differences in the cortex, midbrain, and thalamus (Alkire et al., 1995; Alkire et al., 1997; Alkire, 1998; Alkire et al., 1999; Alkire et al., 2000; Veselis et al., 1997).

The neurons of the thalamus mediating arousal and nociception have been identified as loci for the effects of general anesthetics, as well as the cortex, thalamic relay neurons, and diffuse thalamic projection neurons (Antognini et al., 2000). Functional magnetic resonance imaging has also been applied to studying the effects of anesthetic induction, showing reduced auditory cortex activity with increased anesthetic depth, however with primary auditory cortex remaining active after loss of consciousness (Hall et al., 2000). A recent study reported the effects of general anesthesia on intracranial neural data recorded from the thalamus and frontal cortex, and demonstrated that frontal EEG activity is predictive of loss of consciousness while thalamic LFP activity is predictive of movement. In the rat, one study found that septal-hippocampal activity in the gamma (30-50 Hz) band predicted movement following general anesthesia. In rats, reduction in theta (4-12 Hz) oscillations in the hippocampus were associated with anesthesia (Angel, 1991). These studies provide some evidence for the region-specific effects of anesthesia, but imaging studies have not shown direct functional changes in sensory, nociceptive, associational, or cognitive systems as a result of anesthesia.

The results of some fMRI studies, using both observational and stimulus-driven paradigms, present an interpretation challenge, because the inhaled anesthetics are vasodilators, “washing out” the blood oxygen level dependent (BOLD) signal (Logothetis et al., 1999). The recent study by Purdon et al. (2009) used an anesthetic induction with propofol, which is a minimal vasodilator, and maintained an adequate airway throughout the study.

Staging of Anesthetic Depth using EEG

The characteristic stages of general anesthesia were first reported by Guedel in 1937 (Calverley, 1989). The stages described in current clinical practice are the same as those reported by Kiersey in 1951 (Figure 1). Each stage is associated with characteristic EEG patterns as well as clinically observable behaviors. Almost all general anesthetic agents produce these stereotyped stages.

Stage 1, the induction or analgesic stage, occurs at low doses. Anesthetics typically increase EEG beta power (12-20 Hz). The patient experiences dizziness, decreased sensitivity to touch and pain, increased sense of hearing, and increased response to auditory stimuli. Blood pressure is normal and pulse is irregular.

Stage 2, the excitement or paradoxical excitation stage, occurs as dose increases. Beta power in the EEG is replaced by increased alpha power (8-12 Hz) that shifts anteriorly. The patient may experience muscular activity and delirium. Pulse is irregular and fast, and blood pressure is high.

Stage 3, the surgical or operative stage, occurs as yet higher doses. Bispectral coupling between low and high frequencies is observed in the EEG, and gamma-band coherence (26-70

Hz) increases. Pulse is steady and slow, and blood pressure is normal. Airway management is required.

Stage 4, the deepest level of anesthesia, is observed at the highest anesthetic doses delivered clinically. Characteristic EEG activity of this stage includes burst suppression patterns, isoelectricity, and spindles. The spindles of stage 4 EEG have characterized been shown to have different properties from those in Stage 2 sleep, however they have not been studied in the same subject. In this stage, pulse is weak and thready, and blood pressure is low. The risk for POCD induced by hypoxia is at greatest risk in Stage 4. (Stanski, 2000).

The functional significance of the anesthesia-related EEG patterns at each stage is not known. A priority for anesthesia research is to identify the brain networks responsible for these signals in relation to sensory, cognitive, memory, and pain systems, and also to better characterize the onset of the EEG stages and their behavioral correlates for improved anesthetic monitoring.

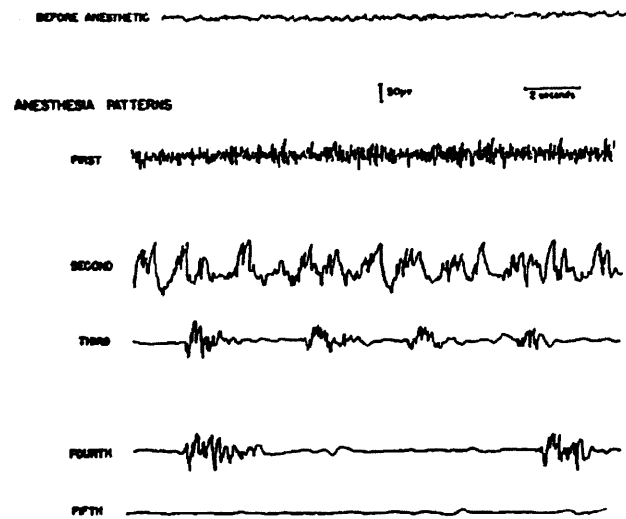


FIG. 1.
Electro-encephalographic patterns in deepening thiopental anaesthesia.

Figure 1. Stages of anesthesia EEG reported in Kiersey, 1951.

Clinical Monitoring of Anesthetic Depth

In clinical practice, depth of anesthesia is primarily monitored using easily observed behavioral and physiological indicators rather than electronic monitoring systems. These indicators include loss of response to verbal and tactile stimuli, heart rate, blood pressure, pupil size, and lash reflex. Loss of response to noxious stimuli has been quantified experimentally in terms of pharmacological EC50 points, and such points are used as a guideline for anesthetic dosage. One such reference point is the Minimum Alveolar concentration (MAC), the concentration at which 50% of patients can be expected to be unconscious (Eger et al., 1965; Quasha et al., 1980; Stanski, 2000).

The EEG has been the primary neurophysiological recording used to measure and characterize neural activity related to anesthetic induction. EEG-based anesthesia monitors exist,

such as the Bispectral Index (BIS). Such monitors reduce a number of EEG-based characteristics to a single parameter that can be used by anesthesiologists to guide drug delivery. (Rampil, 1998). While early studies showed that monitors like the BIS could improve patient recovery time and reduce quantity of delivered drugs, in practice the observation of behavioral and physiological variables is typically used as the main indicator of anesthetic depth (John et al., 2001). Furthermore, the recent B-Unaware clinical trial demonstrated that standard anesthesia monitors are ineffective in reducing post-operative recall compared with a standardized inhaled anesthetic protocol. Improvements in EEG-based monitoring have the potential to reduce anesthetic morbidity; it has been shown that reduced post-operative pain and decreased recovery time may be achieved by selecting an appropriate anesthetic dose (Ghoneim and Block, 1997).

Relationship with Sleep, Coma, and Epilepsy

The behavioral state of anesthesia has both similarities and differences with other behavioral states associated with loss of consciousness: sleep, coma, and portions of the epileptic seizure. It is well known that the state of general anesthesia differs functionally from these other behavioral states. Despite the differences between anesthesia and other unconscious states, burst suppression patterns are similarly observed in coma, epilepsy, and anesthesia, and EEG spindles are observed in both Stage 2 sleep and anesthesia (Antkowiak, 1999). The comparison of EEG patterns in sleep and anesthesia, in particular as recorded from a variety of regions, would be informative about the neural dynamics underlying unconscious states in both settings. A comparison of burst suppression patterns in anesthesia and coma may be informative to assess the integrity of cortical function during hypoxic coma and other neurological disorders.

Aims of the thesis

The goal of this thesis was to establish neural correlates of anesthesia that can be used for improved anesthetic monitoring and drug administration. Furthermore, the goal was to increase scientific understanding of the neural activity underlying the state of general anesthesia in relation to sensory, cognitive, memory, and pain systems. Epilepsy patients who have been previously implanted with intracranial electrodes present an advantageous opportunity to record neural activity from the deep structures of the brain, in a way that is regionally distributed, temporally precise, and relevant to clinical practice. This thesis constitutes two analyses performed on a set of data that we obtained from 14 such patients.

In the first analysis, we characterized the properties and dynamics of electrophysiological signals during anesthetic induction as obtained in surface recordings and intracranial EEG signals. We performed spectral analysis to quantify and analyze the frequency content, amplitude, onset, and cessation of the stage-specific signals and compared these metrics across subjects and electrode channels. In particular, we determined the alpha frequency, and functional neuroanatomical regions and networks where the characteristic alpha signals of anesthesia could be observed. We also tested the hypothesis that the spectral characteristics of the signals were correlated with the stimulus parameters of the experiment – including auditory stimuli - and/or with the subjects' behavioral responses. We assessed whether activity before and after loss of consciousness in regions such as auditory cortex, the hippocampus, the parietal lobe, and others may be related to the separable components of anesthesia including analgesia, amnesia, and unconsciousness. In the second analysis, we performed coherence analysis to identify distributed networks of neuronal activity across the medial temporal lobe, cingulate gyrus, temporal cortex, frontal cortex, and white matter tracts. In particular, we related the results to previously reported characteristics of alpha coherence in anesthesia.

References

- Alkire MT (1998) Quantitative EEG correlations with brain glucose metabolic rate during anesthesia in volunteers. *Anesthesiology* 89: 323-333.
- Alkire MT, Haier RJ, Barker SJ, Shah NK, Wu JC, Kao YJ (1995) Cerebral metabolism during propofol anesthesia in humans studied with positron emission tomography. *Anesthesiology* 82: 393-403.
- Alkire MT, Haier RJ, Fallon JH (2000) Toward a unified theory of narcosis: brain imaging evidence for a thalamocortical switch as the neurophysiologic basis of anesthetic-induced unconsciousness. *Conscious Cogn* 9: 370-386.
- Alkire MT, Haier RJ, Shah NK, Anderson CT (1997) Positron emission tomography study of regional cerebral metabolism in humans during isoflurane anesthesia. *Anesthesiology* 86: 549-557.
- Alkire MT, Pomfrett CJ, Haier RJ, Gianzero MV, Chan CM, Jacobsen BP, Fallon JH (1999) Functional brain imaging during anesthesia in humans: effects of halothane on global and regional cerebral glucose metabolism. *Anesthesiology* 90: 701-709.
- Angel A (1991) The G. L. Brown lecture. Adventures in anaesthesia. *Exp Physiol* 76: 1-38.
- Angel A (1993) Central neuronal pathways and the process of anaesthesia. *Br J Anaesth* 71: 148-163.
- Angel A, Arnott RH, Linkens DA, Ting CH (2000) Somatosensory evoked potentials for closed-loop control of anaesthetic depth using propofol in the urethane-anaesthetized rat. *Br J Anaesth* 85: 431-439.
- Angel A, LeBeau F (1992) A comparison of the effects of propofol with other anaesthetic agents on the centripetal transmission of sensory information. *Gen Pharmacol* 23: 945-963.
- Antkowiak B (1999) Different actions of general anesthetics on the firing patterns of neocortical neurons mediated by the GABA(A) receptor. *Anesthesiology* 91: 500-511.
- Antognini JF, Buonocore MH, Disbrow EA, Carstens E (1997) Isoflurane anesthesia blunts cerebral responses to noxious and innocuous stimuli: a fMRI study. *Life Sci* 61: L-54.
- Antognini JF, Carstens E, Sudo M, Sudo S (2000a) Isoflurane depresses electroencephalographic and medial thalamic responses to noxious stimulation via an indirect spinal action. *Anesth Analg* 91: 1282-1288.

- Antognini JF, Schwartz K (1993) Exaggerated anesthetic requirements in the preferentially anesthetized brain. *Anesthesiology* 79: 1244-1249.
- Antognini JF, Wang XW (1999) Isoflurane indirectly depresses middle latency auditory evoked potentials by action in the spinal cord in the goat. *Can J Anaesth* 46: 692-695.
- Antognini JF, Wang XW, Carstens E (2000b) Isoflurane action in the spinal cord blunts electroencephalographic and thalamic-reticular formation responses to noxious stimulation in goats. *Anesthesiology* 92: 559-566.
- Calverley RK (1989) Anesthesia as a specialty: Past, present, and future. In: *Clinical Anesthesia* (Barash PG, Cullen BF, Stoelting RK, eds), pp 3-34. New York: J.B. Lippincott Company.
- Dilger JP (2001) Basic pharmacology of volatile anesthetics. In: *Molecular Bases of Anesthesia* (Moody E, Skolnick P, eds), pp 1-36. New York: CRC Press.
- Duch DS, Vysotskaya TN (2001) Anesthetic modification of neuronal sodium and potassium channels. In: *Molecular Bases of Anesthesia* (Moody E, Skolnick P, eds), pp 201-230. New York: CRC Press.
- Dwyer R, Bennett HL, Eger EI, Heilbron D (1992) Effects of isoflurane and nitrous oxide in subanesthetic concentrations on memory and responsiveness in volunteers. *Anesthesiology* 77: 888-898.
- Dwyer RC, Rampil IJ, Eger EI, Bennett HL (1994) The electroencephalogram does not predict depth of isoflurane anesthesia. *Anesthesiology* 81: 403-409.
- Eger EI, Saidman LJ, Brandstater B (1965) Minimum alveolar anesthetic concentration: A standard for anesthetic potency. *Anesthesiology* 26: 756-763.
- Fowler KA, Huerkamp MJ, Pullium JK, Subramanian T (2001) Anesthetic protocol: propofol use in Rhesus macaques (*Macaca mulatta*) during magnetic resonance imaging with stereotactic head frame application. *Brain Res Brain Res Protoc* 7: 87-93.
- Franks NP, Lieb WR (1984) Do general anaesthetics act by competitive binding to specific receptors? *Nature* 310: 599-601.
- Franks NP, Lieb WR (1991) Stereospecific effects of inhalational general anesthetic optical isomers on nerve ion channels. *Science* 254: 427-430.
- Franks NP, Lieb WR (1994) Molecular and cellular mechanisms of general anaesthesia. *Nature* 367: 607-614..
- Ghoneim MM, Block RI (1997) Learning and memory during general anesthesia: an update. *Anesthesiology* 87: 387-410.

- Gibbs FA, Gibbs EL, Lennox WG (1937) Effect on the electroencephalogram of certain drugs which influence nervous activity. *Arch Intern Med* 60: 154-169.
- Hall DA, Haggard MP, Akeroyd MA, Palmer AR, Summerfield AQ, Elliott MR, Gurney EM, Bowtell RW (1999) "Sparse" temporal sampling in auditory fMRI. *Hum Brain Mapp* 7: 213-223.
- Hall DA, Haggard MP, Akeroyd MA, Summerfield AQ, Palmer AR, Elliott MR, Bowtell RW (2000a) Modulation and task effects in auditory processing measured using fMRI. *Hum Brain Mapp* 10: 107-119.
- Hall DA, Summerfield AQ, Goncalves MS, Foster JR, Palmer AR, Bowtell RW (2000b) Time-course of the auditory BOLD response to scanner noise. *Magn Reson Med* 43: 601-606.
- Hemmings HC (2001) Volatile anesthetic effects on calcium channels. In: *Molecular Bases of Anesthesia* (Moody E, Skolnick P, eds), pp 147-178. New York: CRC Press.
- Hoge RD, Atkinson J, Gill B, Crelier GR, Marrett S, Pike GB (1999a) Investigation of BOLD signal dependence on cerebral blood flow and oxygen consumption: the deoxyhemoglobin dilution model. *Magn Reson Med* 42: 849-863.
- Hoge RD, Atkinson J, Gill B, Crelier GR, Marrett S, Pike GB (1999b) Linear coupling between cerebral blood flow and oxygen consumption in activated human cortex. *Proc Natl Acad Sci U S A* 96: 9403-9408.
- Janicki PK (2001) Inhalational anesthetic effects of neuronal plasma membrane Ca^{2+} -ATPase. In: *Molecular Bases of Anesthesia* (Moody E, Skolnick P, eds), pp 179-200. New York: CRC Press.
- John ER (2001) A field theory of consciousness. *Conscious Cogn* 10: 184-213.
- John ER, Prichep LS, Kox W, Valdes-Sosa P, Bosch-Bayard J, Aubert E, Tom M, diMichele F, Gugino LD (2001) Invariant reversible QEEG effects of anesthetics. *Conscious Cogn* 10: 165-183.
- Moody E, Skolnick P (2001) *Molecular Bases of Anesthesia*. New York: CRC Press.
- Moody E, Skolnick P (2001) Neurochemical actions of anesthetics at the GABA_A receptors. In: *Molecular Bases of Anesthesia* (Moody E, Skolnick P, eds), pp 273-288. New York: CRC Press.
- Pearce RA (2001) Effect of volatile anesthetics on GABA_A receptors: Electrophysiologic studies. In: *Molecular Bases of Anesthesia* (Moody E, Skolnick P, eds), pp 245-272. New York: CRC Press.

- Prys-Roberts C (1987) Anaesthesia: a practical or impractical construct? *Br J Anaesth* 59: 1341-1345.
- Quasha AL, Eger EI, Tinker JH (1980) Determination and applications of MAC. *Anesthesiology* 53: 315-334.
- Rampil IJ (1994) Anesthetic potency is not altered after hypothermic spinal cord transection in rats. *Anesthesiology* 80: 606-610.
- Rampil IJ (1998) A primer for EEG signal processing in anesthesia. *Anesthesiology* 89: 980-1002.
- Rampil IJ, Mason P, Singh H (1993) Anesthetic potency (MAC) is independent of forebrain structures in the rat. *Anesthesiology* 78: 707-712.
- Skolnick P, Moody E (2001) Stereoselective actions of volatile anesthetics. In: *Molecular Bases of Anesthesia* (Moody E, Skolnick P, eds), pp 289-304. New York: CRC Press.
- Stanski DR (2000) Monitoring depth of anesthesia. In: *Anesthesia* (Miller RD, ed), pp 1087-1116. Philadelphia: Churchill Livingstone.
- Veselis RA, Reinsel R, Alagesan R, Heino R, Bedford RF (1991) The EEG as a monitor of midazolam amnesia: changes in power and topography as a function of amnesic state. *Anesthesiology* 74: 866-874.
- Veselis RA, Reinsel RA, Beattie BJ, Mawlawi OR, Feshchenko VA, DiResta GR, Larson SM, Blasberg RG (1997) Midazolam changes cerebral blood flow in discrete brain regions: an H₂(¹⁵O) positron emission tomography study. *Anesthesiology* 87: 1106-1117.

Chapter 2: Intracranial correlates of anteriorization during propofol general anesthesia

Abstract

More than 25 million Americans receive general anesthesia (GA) each year and stereotyped signatures of general anesthesia in the electroencephalogram (EEG) have been known since the 1930's. One such signature is a change in the distribution of alpha (8-13 Hz) power in the electroencephalogram from a posterior distribution in the awake state to an anterior distribution in the unconscious state. The intracranial correlates of this effect observed in EEG are not well understood.

This study examined neural recordings from 14 patients who had been previously implanted with intracranial depth electrodes, some of whom also had EEG surface electrodes, while those patients were induced with propofol general anesthesia. We show that anteriorization of alpha power during general anesthesia is associated with two distinct phenomena.

The first phenomenon is a disruption of traditional waking alpha oscillations which include the occipital, sensorimotor, and auditory alpha rhythms. We demonstrate that two of the rhythms – sensorimotor and auditory – are related to task in the data set and are disrupted at loss of consciousness. The second phenomenon is of the onset of de novo alpha oscillations in frontal and midline structures including the cingulate cortex, hippocampus, and frontal white matter. We provide evidence of distinct generators for hippocampal and frontal alpha rhythms during general anesthesia.

Introduction

Each year, more than 25 million patients receive general anesthesia (GA) in the United States. General anesthesia is a drug-induced, reversible behavioral state that includes five separable components: loss of consciousness, amnesia, loss of pain perception, loss of movement, and hemodynamic stability. While mechanisms of general anesthetics are well understood at a cellular and molecular level, the brain systems and circuits underlying these five separable components of anesthesia are not fully characterized (Brown, Lydic, & Schiff, 2010).

Elucidating the effects of general anesthetics in functional brain regions – such as those regions underlying perception, cognition, and memory – is an important step toward improved anesthetic monitoring. Anesthesia-related morbidity is a significant medical problem: approximately 1 in 500 patients experience postoperative recall (POR) of events during surgery (Liu, Thorp, Graham, & Aitkenhead, 1991), up to 41% of elderly patients experience post-operative cognitive dysfunction (POCD), with long-term deficits found in 13% of such patients (Moller et al., 1998). If the brain systems that underlie general anesthesia are better understood, methods may be devised to independently monitor neural activity in these networks and guide drug administration. In addition to having clinical importance, a systems level explanation of general anesthesia may lead to a better understanding of sleep, coma, and the conscious state.

Electrophysiologic signatures of general anesthesia demarcating loss and recovery of consciousness have been established in humans (Breshears et al., 2010; Gibbs, F.A., Gibbs & Lennox, 1937; Purdon et al., 2012). One such signature associated with unconsciousness is an anteriorization of power in the alpha frequency band (8-13 Hz) that occurs in the electroencephalogram (EEG). This effect was first observed with epidural electrodes in monkeys (Tinker, Sharbrough, & Michenfelder, 1977) and has been replicated in human EEG (Feshchenko, Veselis, & Reinsel, 2004). The intracranial correlate of this effect observed in EEG is unknown.

While, in general anesthesia, EEG alpha dynamics are a reliable marker of loss of consciousness, in the waking state, alpha dynamics are functionally correlated with sensorimotor behavior, cognition, vision and sleep (Niedermeyer E., 1997). Three distinct alpha rhythms have been observed in recordings from the human cortex. The occipital or traditional alpha rhythm is recorded from occipital cortex and is suppressed when the eyes are open (Andersen, 1968). The sensorimotor mu or wicket rhythm is recorded from somatomotor cortex and is suppressed during sensorimotor execution or preparation (Kuhlman, 1978). The third or tau rhythm is recorded from over a broad region of temporal cortex that includes auditory cortex, and is thought to be suppressed during auditory or cognitive stimuli (Lehtelä, Salmelin, & Hari, 1997). Tau can not readily be identified in surface EEG and must be recorded from intracranial electrodes. These three rhythms are distinct in their distribution over cortex, frequency content, task responsiveness, development in mammals, and relationship with disease states. Suppression of alpha power during sensation, imagery, planning, and execution during sensorimotor tasks is a general principle of the phenomenology of this oscillation in its three forms (Niedermeyer E., 1997).

Alpha rhythms during GA, as well as wakefulness, sleep and coma, are thought to occur as a result of neuronal activity in both thalamo-cortical and cortico-cortical networks (Brown et al., 2010; Hughes & Crunelli, 2005; Lopes da Silva, Vos, Mooibroek, & van Rotterdam, 1980). A computational model of alpha frequency dynamics with the anesthetic agent propofol (2,6-diisopropylphenol) suggests that these rhythms are mediated by thalamo-cortical circuits, with propofol strengthening reciprocal projections between cortical pyramidal cells and thalamocortical relay neurons (Ching, Cimenser, Purdon, Brown, & Kopell, 2010). Ching et al. have proposed that localized patterns of alpha band changes during GA may be the result of

differential effects of propofol on distinct thalamic nuclei. The prediction of increased anterior alpha power and coherence during unconsciousness have been confirmed in high density EEG studies (Cimenser et al., 2011). Such studies have also established the result that alpha and slow (0.1 – 1 Hz) frequency EEG dynamics are tightly coupled after propofol (Mukamel et al., n.d.; Purdon et al., 2012), and that the phase of this relationship varies systematically with anesthetic depth. However, the mechanisms of alpha and slow frequency coupling are not well understood.

In this report, we examine intracranial neural recordings in a set of human patients, some of which have surface EEG, so we can establish neurophysiological correlates of alpha power anteriorization during the transition to unconsciousness with propofol. These human subjects have been previously implanted with intracranial electrodes for management of intractable epilepsy. Extending the results of previous research that has been performed with subdural electrode arrays resting on the cortical surface (Breshears et al., 2010), the electrodes in this data set include depth electrode arrays penetrating into cingulate cortex, hippocampus, and medial white matter. This allows us to record from cortical and subcortical regions that are distant from surface EEG and may be related to the behavioral components of GA.

We hypothesize that anteriorization of EEG alpha power is associated with disruption of the three dominant alpha band rhythms in human cortex: traditional occipital alpha, sensorimotor mu and temporal tau. Moreover, we hypothesize that anteriorization is associated with *de novo* alpha dynamics in anterior brain regions that do not have a dominant EEG alpha rhythm observable in the waking or sleep states. Previous research has pointed to a role for anterior cingulate cortex as a site of anesthesia induced PET activation changes (Schlunzen et al., 2011). The frequency specific effects of propofol in anterior white matter, prefrontal cortex, cingulate cortex, and subcortical regions including hippocampus are not known. We examine power dynamics in the

alpha frequency band at these recording sites, and discuss the implications for systems and network level mechanisms of general anesthesia.

Figure 1. (A) Photograph of an 8x8 grid array of platinum iridium electrodes (*Ad-Tech*), shown with a U.S. quarter for size comparison. Intraoperative photograph of a craniotomy (left) and overlaid electrode array (right). (B) Sagittal maximum-intensity projection of a subdural grid electrode array in a postoperative CT scan. (C). Linear penetrating depth electrode array (*Ad-Tech*). (D). Coronal maximum-intensity projection of a depth electrode array in a postoperative CT scan.

Materials and Methods

Data collection. 14 patients were implanted with iEEG electrode arrays as part of standard clinical treatment for intractable epilepsy. The arrays included linear penetrating depth arrays having 6-8 electrodes, subdural grid arrays having 16-64 electrodes, and/or subdural strip arrays having 4-16 electrodes (*Adtech Medical, Racine, WI*) (Figure 1). Surface EEG electrodes were additionally applied to six patients in a subset of the standard 10-20 EEG configuration. Electrode placement was selected by the patients' clinicians without regard to the current study and is summarized in Figure S1. Patient demographic and clinical information are provided in Table 1. All patients gave informed consent in accordance with protocols approved by the hospital's Institutional Review Board.

Recordings were obtained during electrode explant surgery that occurred after 1-3 weeks of inpatient monitoring to determine epileptogenic foci. Signal acquisition began prior to induction

of general anesthesia and continued until the electrodes were disconnected for explant. EEG and iEEG signals were recorded with a sampling rate of a 2000, 500, or 250 Hz depending on settings of the hospital's clinical acquisition system. Signals were digitized with hardware amplifiers (*XLTEK, Natus Medical, Inc., San Carlos, CA*) that bandpassed between 0.3 Hz and the sampling rate, and were stored on a computer (*Dell*) for offline processing. A linked earlobe electrode (A1-A2), a C2 reference on the back of the neck, or an inverted disc electrode on the inner skull table were used as a reference when available; otherwise an average reference was used (N=1, patient 13).

TABLE 1. Patient clinical and demographic information.

Anesthesia. All patients underwent induction of general anesthesia with propofol. 13 patients received a bolus dose; one patient received an infusion (patient 2). Drug protocols were selected by the patients' clinicians without regard to the current study.

Behavioral task. Patients were delivered auditory stimuli through headphones (prerecorded words and the patient's name) approximately every 4 seconds during the task, and were instructed to respond with a button click. Responses were recorded using stimulus presentation software (*Presentation, Neurobehavioral Systems, Inc., Albany, CA*, or *EPrime, Psychology Software Tools, Inc., Sharpsburg, PA*). Loss of consciousness time (LOC) was defined as the time of the first stimulus to which the patient did not respond. One patient was excluded from performing the auditory task by request of his clinician (patient 10). LOC was defined marked at 30 seconds after propofol bolus dose for that patient for display in exemplar figures. This patient was excluded from group analyses of peri-LOC dynamics.

Electrode localization. A postoperative CT scan and preoperative T1-weighted MRI scan were obtained for each patient. Data were processed using open-source software (Freesurfer, <http://surfer.nmr.mgh.harvard.edu/fswiki>) and custom programs written in MATLAB (*The Mathworks Inc., Natick, MA*). Coregistration of postoperative CT to preoperative MRI was computed using automated routines in Freesurfer and verified visually. RAS coordinates were identified for all iEEG electrodes in the subject's anatomical space by visual inspection of a maximal intensity projection of the CT (Figure 1). Those coordinates were projected to the subject's preoperative MRI space using coregistration matrices. An automatic rendering of the cortical surface was created from the preoperative MRI image. RAS coordinates of electrodes from subdural grid and strip arrays were mapped to the closest coordinate on the rendered cortical surface using a minimum energy procedure (Dykstra et al, 2010). Average cortical surface renderings and MRI volumes were computed as well as transformation matrices between each patient's coordinate system and the group average coordinate systems.

Anatomical mapping. Electrode coordinates were automatically mapped to anatomical labels as described in (Fischl et al., 2002, 2004). Cortical parcellation labels were used for grid and strip electrode arrays and volumetric segmentation labels were used for depth electrode arrays. Segmentation and parcellation results were examined visually on the MRI image at each electrode location and spurious results were removed from the data set ($n < 5\%$). Functional segmentations were determined from a subset of the structural segmentations, including functional segmentations for the primary auditory cortex, primary somatosensory cortex, primary motor cortex, cingulate cortex, hippocampus, and white matter. Remaining electrodes were segmented into broader anatomical regions due to a smaller number of electrodes outside of those regions previously listed. Occipital, parietal, and inferotemporal cortex were combined,

and frontal and orbitofrontal cortex were combined, and temporal cortex (non-auditory) was labeled. These subdivisions were selected to include only grey matter. Unsegmented regions as well as subcortical regions comprising fewer than three channels in the data set were excluded from further analysis.

Data exclusion. Individual electrodes with recordings predominated by artifacts (absent signal or amplitude $>10\times$ the array median) were excluded from analysis by visual inspection. Shorter segments of data in the remaining electrodes were excluded using the same criteria. Individual electrodes or shorter segments of data were excluded that contained epileptiform discharges, determined by visual inspection. Total time of removed segments was $<5\%$. In one patient, 78/80 channels were removed due to generalized epileptiform discharges (patient 44). In one patient, 16 channels were removed due to the appearance of dysplastic cortex in the MRI (patient 8).

Data analysis. In each subject, two epochs were distinguished over the recording period. The preinduction epoch began at a period of time 400 to 150 seconds prior to loss of consciousness. The start time for this epoch was chosen such that the preinduction recording time was approximately 150 seconds in most channels when large recording artifacts were removed. The preinduction epoch ended at the time of the first dose of propofol. We used visual inspection to identify the postinduction epoch. This epoch defined a period of stationary spectral power that occurred after characteristic paradoxical excitation and prior to burst suppression in the five patients who underwent burst suppression. Burst suppression intervals were excluded to avoid the confound of low-power suppression intervals in group analyses, which differed in total time across patients. The post-induction epoch ended at any of these events: a) the first suppression period apparent in the median spectrogram, b) the delivery of any anesthetic drug besides propofol, and c) the end of the recording. The stationary post-induction epoch was identified by

visual inspection of the median spectrogram computed across all channels, was identified prior to further analyses, and was verified by an anesthesiologist (E.B.¹). The epochs are indicated in the exemplar figures for each patient.

Retained signals were low-pass filtered at 100 Hz and resampled at 250 Hz using finite impulse response filters, and spectrograms were computed for each channel with Chronux software. Spectrograms were computed with 3 tapers, 2 second windows, 1 Hz frequency resolution, and .2 second time steps. For display, raw time-series were lowpass filtered below 40 Hz using finite impulse response filters. In all epochs, the median log spectral power between 8-13 Hz was computed for each electrode as the median over spectrogram windows in the epoch and mean over frequency bins in the alpha band.

A modulation index was computed to describe the relationship between slow oscillation (0.1 to 1 Hz) phase and the alpha oscillation amplitude for all channels. The index was computed as described in (Tort, Komorowski, Eichenbaum, & Kopell, 2010) with 12 phase bins, 10 seconds of time in each phase bin. The analytic phase value extracted using a Hilbert transformation of a signal bandpassed using FIR filters of length 4500 with passbands of 7.5-13.5 Hz for the alpha band, and 0.1-1Hz for the slow band, with transition bandwidths of 10% or 0.5 Hz, whichever was smaller. To display alpha band amplitude concurrently with an iEEG trace by coloring the trace relative to amplitude, alpha amplitude was normalized to a percentile of the amplitude at all time points over the time period of the displayed trace.

To ascertain task-related modulations of alpha power in each recorded channel, an event related spectral perturbation (ERSP) was computed for each channel in which amplitude in the alpha band was related to auditory stimuli both before and after LOC and button presses prior to LOC.

¹Note: epoch times were verified when E.B. observed each figure during our meeting in September 2012.

Alpha amplitude was computed as described above in order to have a metric with temporal resolution the same as the sampling rate. A window of [-.75 to 1.5] seconds was computed around each event time, with the first 0.5 seconds of the window assigned as a baseline. Each window was normalized by removing its mean. Mean normalized alpha amplitude was then computed for each point across the 2.25 second window, and values that was significantly different from the mean amplitude in the baseline window were ascertained for each time point in the window. Significance was computed using 500 iterations of a surrogate control of shuffled times perturbed uniformly over +/- 4 seconds. A significance level of $\alpha=0.05$ was computed obtained at every point in the perievent window outside of the baseline and a familywise error rate was used to correct for multiple comparisons. No corrections were made over multiple electrodes.

Results

Between 54 and 124 channels were recorded in each patient. Intracranial neural recordings were obtained at 1521 recording sites from 14 patients. Seven of those patients also had surface EEG. Five subjects demonstrated burst suppression EEG.

Characteristic waking alpha rhythms are abruptly suppressed and *de novo* alpha rhythms emerge at LOC

Figure 2 shows spectrograms of iEEG signals (right panel) that were recorded in several cortical and subcortical regions (localization in left panel) for Patient 9, who had concurrent iEEG and surface EEG. Prior to LOC, an alpha rhythm is observed observed in the posterior bipolar surface EEG channel, which is simultaneous with an iEEG alpha rhythm recorded in the occipital cortex subdural electrode. This oscillation is consistent with the traditional occipital alpha rhythm because of its spatial location, high power relative to other frequencies and

channels, and frequency content. In this patient, a temporal alpha oscillation occurs also in the medial temporal cortex that is spatially consistent with a tau rhythm and occurs with a greater peak frequency in the alpha band over the preinduction epoch (8.7 Hz in the occipital channel and 10.1 Hz in the temporal channel), which may indicate distinct rhythms. Alpha power in both channels is suppressed abruptly within 10 seconds after LOC.

After LOC, novel alpha rhythms with two distinct phenomenologies are seen in this set of exemplars. An alpha band rhythm appears with a bursting pattern in all channels and with greatest strength in the cingulate cortex recording. The same pattern is seen in both the anterior and posterior surface EEG. A broadband rhythm in the hippocampus between slow frequencies (0.1-1Hz) and high beta / low alpha frequencies (11-13 Hz) emerges after LOC. The phenomena in this subject's exemplars in temporal cortex, cingulate cortex, hippocampus, occipital cortex, and surface EEG are similar to those observed in all other subjects in the data set (Supplementary Figures).

Panel B shows alpha power dynamics across LOC in all of the iEEG electrodes for this patient. Greatest alpha power prior to LOC (top row) occurs in occipital electrodes, and least power is in the cingulate cortex. The distribution is reversed after LOC. A similar distribution is seen in all the other subjects in the data set.

Figure 3 shows spectrograms from exemplar recordings from patient 3, which demonstrate one feature not visible in the first patient's exemplars due to a different distribution of recording sites. In patient 3, a spectrogram from a motor cortex electrode shows activity consistent with the sensorimotor mu oscillation, which has been shown to occur at a higher frequency than occipital alpha and to be concurrent with beta power. In this recording, alpha power at a different frequency band occurs in the motor cortex after LOC, unlike in the auditory and visual cortex

recordings in this and the previous patient. This result in motor and sensorimotor cortices is observed in numerous subjects, which may suggest a distinct behavior in sensorimotor mu producing sites and occipital alpha and temporal tau producing sites.

FIGURE 2. Exemplar spectrograms during propofol anesthesia, patient 9. Region specific changes in alpha power were observed during the transition to GA with propofol. (A), right panels, multitaper spectrograms computed as described in *Materials and Methods* from the signal recorded in exemplar electrodes from a single patient. Dashed line indicates LOC, arrows indicate propofol boluses. Pre-induction and post-induction epochs are indicated below the spectrograms. Right panels, segments of time series from the same recordings. (B), top panel, average alpha band power during the pre-induction epoch at each recording site in a single patient. If the patient was implanted with depth electrode arrays, locations are overlaid on transparent renderings of the patient's brain. If the patient was implanted with strip and grid electrodes arrays, locations are overlaid on cortical surface renderings. If surface EEG was recorded from the patient, electrode locations are shown on a head plot. The exemplar electrodes from panel (A) are indicated on each rendering. Bottom panel, average alpha band power during post-induction epoch as pictured for the pre-induction epoch.

FIGURE 3. Exemplar spectrograms during propofol anesthesia, patient 3.

Anteriorization of the EEG occurs with medialization and anteriorization of the iEEG

Figure 4 shows a region-specific summary of the alpha power change during anesthesia. Median alpha power in the postinduction period is consistently increased in the hippocampus and cingulate cortex, as well as in medial white matter electrodes, by approximately 5 dB. Power is also consistently decreased in a broad region including occipital cortex, parietal cortex, and inferotemporal cortex, as well as in the primary auditory cortex. Activity in motor cortex,

somatosensory cortex, and frontal gray matter increases in some channels and decreases in others. This pattern reflects a medialization of alpha power in the iEEG that is concurrent with the traditional anteriorization in EEG.

FIGURE 4. Region-specific alpha power change during induction of propofol general anesthesia. Change in median alpha frequency power (dB) is overlaid on transparent renderings of the data set average brain. Each circle is a single electrode location for one patient; electrode locations from all patients are plotted together for each functional region. Change in power is computed as the median power in the post-induction period minus median power in the pre-induction period.

A novel alpha oscillation in hippocampus during propofol general anesthesia

In all patients with electrodes in hippocampus a novel broadband rhythm including the alpha

frequency was observed within +/- 30 seconds around LOC. Like the fronto-medial alpha rhythms that occurred in the post-induction period, this novel hippocampal oscillation of propofol GA had an onset tightly linked with unconsciousness. However, the rhythm had several properties that distinguished it from the other alpha rhythms of GA and waking and these were consistent across all subjects. The hippocampal alpha rhythm was broadband, with nearly uniform power from slow (0.1-1) to alpha or low beta frequencies. This rhythm was less coupled to slow oscillation phase than in the signals recorded from locations in other cortical and subcortical regions (Figure 5). The rhythm persisted during suppression periods of burst suppression.

Figure 5. During propofol GA, hippocampal alpha oscillations are distinct from anterior alpha oscillations with respect to slow oscillation coupling and presence during suppression periods of burst suppression. (A), exemplar time series recorded simultaneously from hippocampal and frontal electrodes during the post-induction

period in patient 7. Pseudo-coloring of the iEEG traces alpha amplitude at that time point (see *Materials and Methods*). Alpha power is strongly phase locked to a slow oscillation in the exemplar frontal channel but not in the hippocampal channels in these. (B), phase amplitude coupling illustrated in a phasegram (see *Materials and Methods*) during the pre- and post- induction period in those same channels. (C), spectrograms and time series recorded during burst suppression in an exemplar subject, showing persistence of alpha band activity during suppressions in the hippocampus.

Changes in alpha power are tightly linked with timing of LOC

The exemplar figures show changes in an alpha oscillation that is tightly linked within +/- 30 seconds to loss of responsiveness. In some patients (patients 1 and 3), the offset of an occipital alpha oscillation was most closely temporally linked with LOC and the onset of cingulate and hippocampal rhythms occurred after LOC while in others the pattern was reversed (patient 5). In all patients demonstrating mu and tau oscillations before induction of anesthesia, these oscillations were no longer significantly related to timing of stimuli after induction of anesthesia (Figure 6).

FIGURE 6. Disruption of functional alpha rhythms at LOC. Left panel shows a pseudo-colored iEEG trace from two channels where trace color indicates alpha frequency amplitude at that time point. Black lines (top) indicate responses during the auditory task, and magenta lines (bottom) indicate stimuli. Right panels show event related sensory spectral perturbations in the alpha band in a window around stimulus times. The top pattern is consistent with a mu oscillation in which alpha power is suppressed during sensorimotor response, which occurs ~1sec after stimulus onset. The bottom pattern is consistent with a tau oscillation in which alpha power is suppressed during auditory stimulus. Green lines indicate significant differences from baseline. Both ERSP effects in the alpha band disappear immediately at LOC.

Discussion

We have examined human intracranial and EEG neural recordings during the transition to unconsciousness with propofol bolus, and demonstrated a) a disruption of the occipital, tau, and mu alpha rhythms of wakefulness within seconds surrounding LOC, and b) an emergence of *de novo* alpha frequency rhythms in the hippocampus and frontal midline structures including

cingulate cortex, orbitofrontal and prefrontal cortex, and frontal white matter that are not observed in typical wakefulness. The distribution of changes in alpha power in the occipital lobe, auditory cortex, somatomotor cortex, hippocampus, and frontal midline regions were consistent across patients during the transition to unconsciousness in the clinical setting.

Neurophysiological mechanisms of propofol alpha dynamics

The alpha frequency dynamics described here are in accordance with current thalamocortical hypotheses of alpha anteriorization with propofol (Ching et al., 2010; Purdon et al., 2012). We showed increased alpha power after LOC in anterior midline channels in cingulate cortex, frontal, prefrontal and orbitofrontal cortex, and frontal white matter channels. These regions receive projections from the mediodorsal nucleus of the thalamus (Behrens et al., 2003), which may underlie a common alpha power dynamic driven via common thalamocortical projections .

We observed region-specific differences between propofol's disruptive effects at LOC in the cortical regions that produce occipital alpha, tau, and mu oscillations in waking. In occipital alpha- and tau- producing cortical regions, alpha power was reduced after LOC, while in sensorimotor mu-producing cortical regions, in alpha power was for some patients and channels increased. Several neurophysiological mechanisms may underlie this distinction.

Occipital alpha-, tau-, and mu- producing regions of cortex receive projections from distinct thalamic relay nuclei, with the lateral geniculate nucleus projecting to the occipital cortex, the medial geniculate body projecting to auditory areas, and the ventral nuclei projecting to somatomotor areas (Behrens et al., 2003; Hughes & Crunelli, 2005). Furthermore, the waking alpha rhythms are thought to require connectivity between thalamic reticular neurons and thalamic relay neurons. For the mu rhythm in particular, inhibitory connectivity between reticular and relay nuclei is thought to play an important role in generating the bilaterally

incoherent, focally specific alpha rhythms during sensorimotor tasks (Pfurtscheller & Andrew, 1999). Finally, distinct effects of propofol on GABAergic cortico-cortico circuits may underlie propofol's distinct effects. In specific, cortico-cortical mechanisms are thought to be important in generating the slow cortical potential, which has been shown to gate higher frequency activity after propofol.

A novel hippocampal alpha rhythm with propofol

We have reported a novel broadband rhythm localized to hippocampal channels that includes power in the alpha frequency band, emerges near LOC, persists through the suppression periods of burst suppression, and has slow oscillation coupling properties distinct from the fronto-medial alpha rhythm of propofol GA. Taken together, these features suggest that local hippocampal generators may play be implicated in this rhythm following LOC. Because *in vitro* experiments have not indicated the generation of alpha rhythms with the application of propofol to hippocampal slices while changes in higher frequency gamma oscillations have been shown (Fox & Jefferys, 1998), it can be hypothesized that an intact hippocampus is essential to generate the rhythm. An alternate hypothesis is that the effect has not been observed *in vitro* because of species-specific differences in hippocampal circuitry.

Some properties of this novel rhythm following propofol may be related to neural mechanisms that are functionally significant during waking. If the hypothesis of a local generator of the hippocampal rhythm is confirmed, the result would suggest that GABAergic hippocampal circuits have the capacity to generate oscillations in a broad frequency range, including alpha, and that hippocampal activity may simultaneously reflect locally generated rhythms and thalamically mediated alpha rhythms at distant cortical sites. Such a capacity may be mechanistically relevant to memory encoding and/or retrieval in wakefulness. A role of

hippocampal alpha rhythms in memory processes has been previously reported (Fell et al., 2011; Schürmann, Demiralp, Başar, & Başar Eroglu, 2000) though the effect is less well studied than the role of hippocampal theta in learning and memory. GABAergic circuits in the hippocampus have been implicated in several properties of hippocampal function in the waking state (Banks, White, & Pearce, 2000; Freund & Antal, 1988). The results presented here may inform future biophysical models of human hippocampal circuitry in response to GABA-ergic anesthetic agents in both anesthesia and waking.

The results of this study, in particular with respect to a novel anesthesia-related rhythm in hippocampus, must be interpreted with regards to the dataset of epileptic patients. What is known about GABA-ergic hippocampal networks is consistent with a specific effect in this region. Focal epilepsy. To extend these results, subcortical source localization, animal studies, and Epilepsy may change the results in several ways with respect to normal patients. Activity in the hippocampus may be distinct in power and frequency. We would hypothesize that the broadband, bilaterally coherent properties of this rhythm would be retained. We would hypothesize that the top-edge frequency may be different, or that power may be decreased in normal controls.

Relationship with sleep and coma

The anterior medial pattern of alpha power that we have demonstrated after propofol LOC is not typically observed during sleep. Alpha rhythms that vary with sleep stage have a primarily occipital distribution (McKinney, Dang-Vu, Buxton, Solet, & Ellenbogen, 2011) unlike those we have shown in propofol general anesthesia.

Certain variants of alpha-pattern coma have been described whose power distribution is similar to those we observe in this study (Niedermeyer E., 1997; Young et al., 1994). Postmortem neurohistology in alpha-pattern coma has suggested that widespread cortical, thalamic, and/or

brainstem damage may underlie the fronto-medial power distribution (Westmoreland, Klass, Sharbrough, & Reagan, 1975), which is consistent with current theories of where propofol may act to disrupt GABA-ergic networks.

Relationship with behavioral changes of anesthesia and implications for monitoring

The experimental protocol in this study allowed measurement of loss of responsiveness with a temporal resolution of several seconds. LOC was closely linked to increases in medio-frontal and hippocampal alpha power and decreases in occipital and tau alpha power.

Specific disruption of occipital alpha and auditory tau, and changes in sensorimotor mu oscillations after LOC may be related separable behavioral components of anesthesia: loss of consciousness and akinesia. The disruption of task-related auditory tau oscillations and sensorimotor mu oscillations occurred abruptly within seconds of LOC. The disruptions of these rhythms may be related to the inability to perceive sensory stimuli and perform movements, and may link general anesthesia with disruptions in specific systems-level functional circuits.

The novel broadband rhythm observed in the hippocampus of all subjects may be related to anesthetic-induced amnesia. If the rhythm is related to propofol-induced amnesia, it may provide a novel target for anesthetic monitoring to prevent post operative recall.

References

- Andersen, P. (1968). *Physiological Basis of the Alpha Rhythm*. Plenum Pub Corp.
- Banks, M. I., White, J. A., & Pearce, R. A. (2000). Interactions between distinct GABA(A) circuits in hippocampus. *Neuron*, 25(2), 449-57.
- Behrens, T. E. J., Johansen-Berg, H., Woolrich, M. W., Smith, S. M., Wheeler-Kingshott, C. A. M., Boulby, P. A., Barker, G. J., et al. (2003). Non-invasive mapping of connections between human thalamus and cortex using diffusion imaging. *Nature neuroscience*, 6(7), 750-7. doi:10.1038/nrn1075
- Breshears, J. D., Roland, J. L., Sharma, M., Gaona, C. M., Freudenburg, Z. V., Tempelhoff, R., Avidan, M. S., et al. (2010). Stable and dynamic cortical electrophysiology of induction and emergence with propofol anesthesia. *Proceedings of the National Academy of Sciences of the United States of America*, 107(49), 21170-5. doi:10.1073/pnas.1011949107
- Brown, E. N., Lydic, R., & Schiff, N. D. (2010). I 2638.
- Ching, S., Cimenser, A., Purdon, P. L., Brown, E. N., & Kopell, N. J. (2010). Thalamocortical model for a propofol-induced alpha-rhythm associated with loss of consciousness. *Proceedings of the National Academy of Sciences of the United States of America*, 107(52), 22665-70. doi:10.1073/pnas.1017069108
- Cimenser, A., Purdon, P. L., Pierce, E. T., Walsh, J. L., Salazar-Gomez, A. F., Harrell, P. G., Tavares-Stoeckel, C., et al. (2011). Tracking brain states under general anesthesia by using global coherence analysis. *Proceedings of the National Academy of Sciences of the United States of America*, 108(21), 8832-7. doi:10.1073/pnas.1017041108
- Feshchenko, V. A., Veselis, R. A., & Reinsel, R. A. (2004). Propofol-induced alpha rhythm. *Neuropsychobiology*, 50(3), 257-66. doi:10.1159/000079981
- Fox, J. ., & Jefferys, J. G. . (1998). Frequency and synchrony of tetanically-induced, gamma-frequency population discharges in the rat hippocampal slice: the effect of diazepam and propofol. *Neuroscience Letters*, 257(2), 101-104. ELSEVIER SCI IRELAND LTD. doi:10.1016/S0304-3940(98)00812-X
- Freund, T. F., & Antal, M. (1988). GABA-containing neurons in the septum control inhibitory interneurons in the hippocampus. *Nature*, 336(6195), 170-3. doi:10.1038/336170a0
- Gibbs, F.A., Gibbs, E. L., & Lennox, W. G. (1937). EFFECT ON THE ELECTRO-ENCEPHALOGRAM OF CERTAIN DRUGS WHICH INFLUENCE NERVOUS ACTIVITY. *Archives of Internal Medicine*, 60(1), 154-166. doi:10.1001/archinte.1937.00180010159012
- Hughes, S. W., & Crunelli, V. (2005). Thalamic mechanisms of EEG alpha rhythms and their pathological implications. *The Neuroscientist*: a review journal bringing neurobiology, neurology and psychiatry, 11(4), 357-72. doi:10.1177/1073858405277450
- Kuhlman, W. N. (1978). Functional topography of the human mu rhythm. *Electroencephalography and Clinical Neurophysiology*, 44(1), 83-93. doi:10.1016/0013-4694(78)90107-4

- Lehtelä, L., Salmelin, R., & Hari, R. (1997). Evidence for reactive magnetic 10-Hz rhythm in the human auditory cortex. *Neuroscience letters*, 222(2), 111-4.
- Liu, W. H. D., Thorp, T. A. S., Graham, S. G., & Aitkenhead, A. R. (1991). Incidence of awareness with recall during general anaesthesia. *Anaesthesia*, 46(6), 435-437. doi:10.1111/j.1365-2044.1991.tb11677.x
- Lopes da Silva, F. ., Vos, J. ., Mooibroek, J., & van Rotterdam, A. (1980). Relative contributions of intracortical and thalamo-cortical processes in the generation of alpha rhythms, revealed by partial coherence analysis. *Electroencephalography and Clinical Neurophysiology*, 50(5-6), 449-456. doi:10.1016/0013-4694(80)90011-5
- Moller, J., Cluitmans, P., Rasmussen, L., Houx, P., Rasmussen, H., Canet, J., Rabbitt, P., et al. (1998). Long-term postoperative cognitive dysfunction in the elderly: ISPOCD1 study. *The Lancet*, 351(9106), 857-861. doi:10.1016/S0140-6736(97)07382-0
- Mukamel, E. A., Pirodini, E., Babadi, B., Wong, K. F. K., Pierce, E. T., Harrell, G., Walsh, J. L., et al. (n.d.). A novel transition in brain state during general anesthesia. *In submission*.
- Niedermeyer E. (1997). Alpha rhythms as physiological and abnormal phenomena. *International Journal of Psychophysiology*, 26(1), 19. Elsevier. doi:http://dx.doi.org/10.1016/S0167-8760(97)00754-X
- Pfurtscheller, G., & Andrew, C. (1999). Event-Related changes of band power and coherence: methodology and interpretation. *Journal of clinical neurophysiology* □: *official publication of the American Electroencephalographic Society*, 16(6), 512-9.
- Purdon, P. L., Pierce, E. T., Mukamel, Eran A. Prerau, M. J., Walsh, J. L., Wong, K. F. K., Salazar-Gomez, A. F., Harrell, P. G., et al. (2012). Electroencephalogram Signatures of Loss and Recovery of Consciousness During Propofol-Induced General Anesthesia. *In submission*.
- Tinker, J. H., Sharbrough, F. W., & Michenfelder, J. D. (1977). Anterior shift of the dominant EEG rhythm during anesthesia in the Java monkey: correlation with anesthetic potency. *Anesthesiology*, 46(4), 252-9.
- Tort, A. B. L., Komorowski, R., Eichenbaum, H., & Kopell, N. (2010). Measuring phase-amplitude coupling between neuronal oscillations of different frequencies. *Journal of neurophysiology*, 104(2), 1195-210. doi:10.1152/jn.00106.2010
- Young, G. B., Blume, W. T., Campbell, V. M., Demelo, J. D., Leung, L. S., McKeown, M. J., McLachlan, R. S., et al. (1994). Alpha, theta and alpha-theta coma: a clinical outcome study utilizing serial recordings. *Electroencephalography and clinical neurophysiology*, 91(2), 93-9.

Supplementary Figures

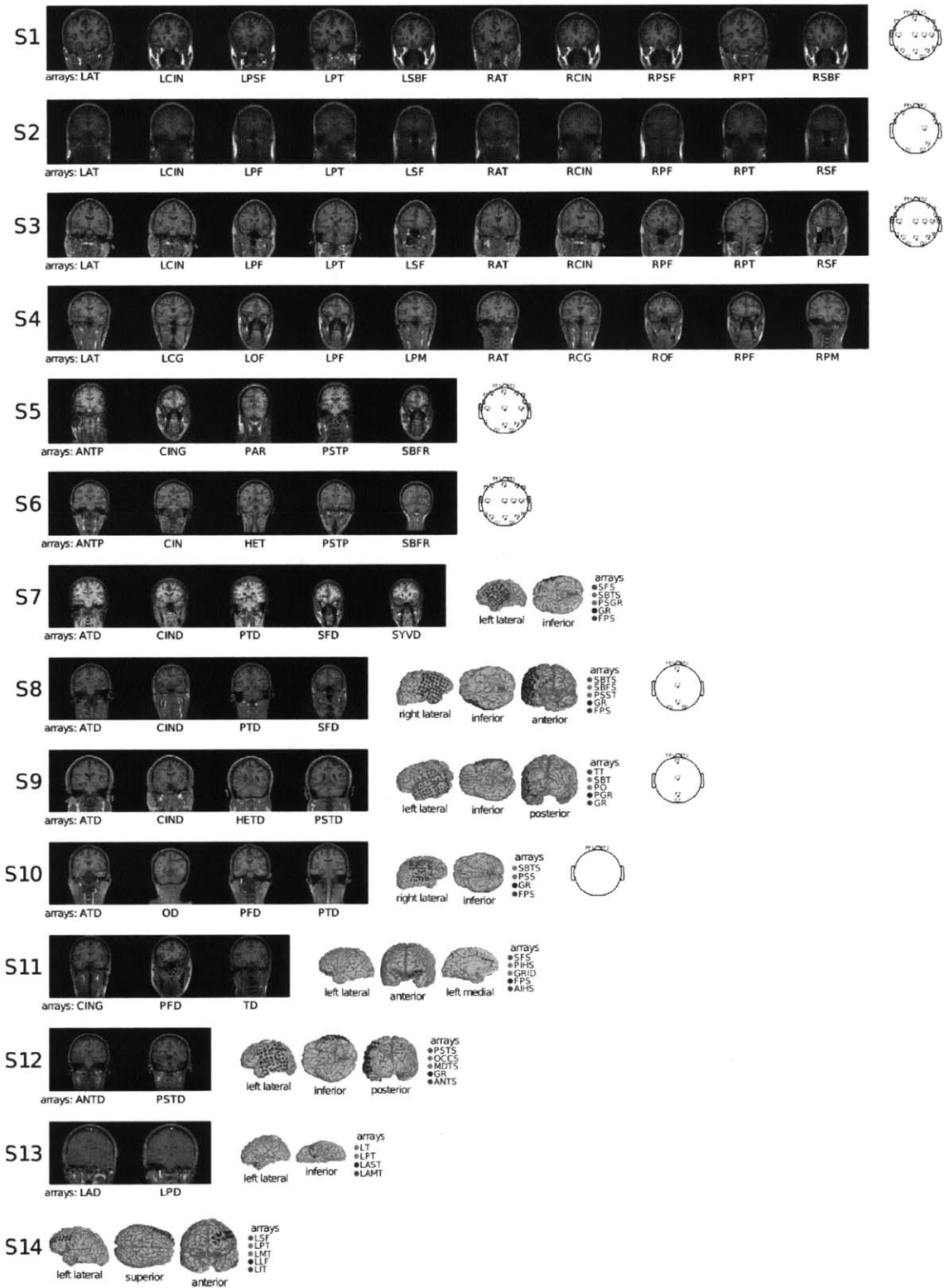


Figure S1 . Electrode coverage for all patients. Leftmost panels show one MRI image for

each depth electrode array, with electrode locations projected onto a semi-coronal slice aligned to the medial and lateral electrode coordinates of the array. Image is shown with the clinical label of the array. R=patient's right side, L=patients' left side. Middle panels show grid and strip electrode array locations overlaid on a rendering of the cortical surface. Rightmost panel shows surface EEG electrodes labeled with positions in the EEG 10-20 International System.

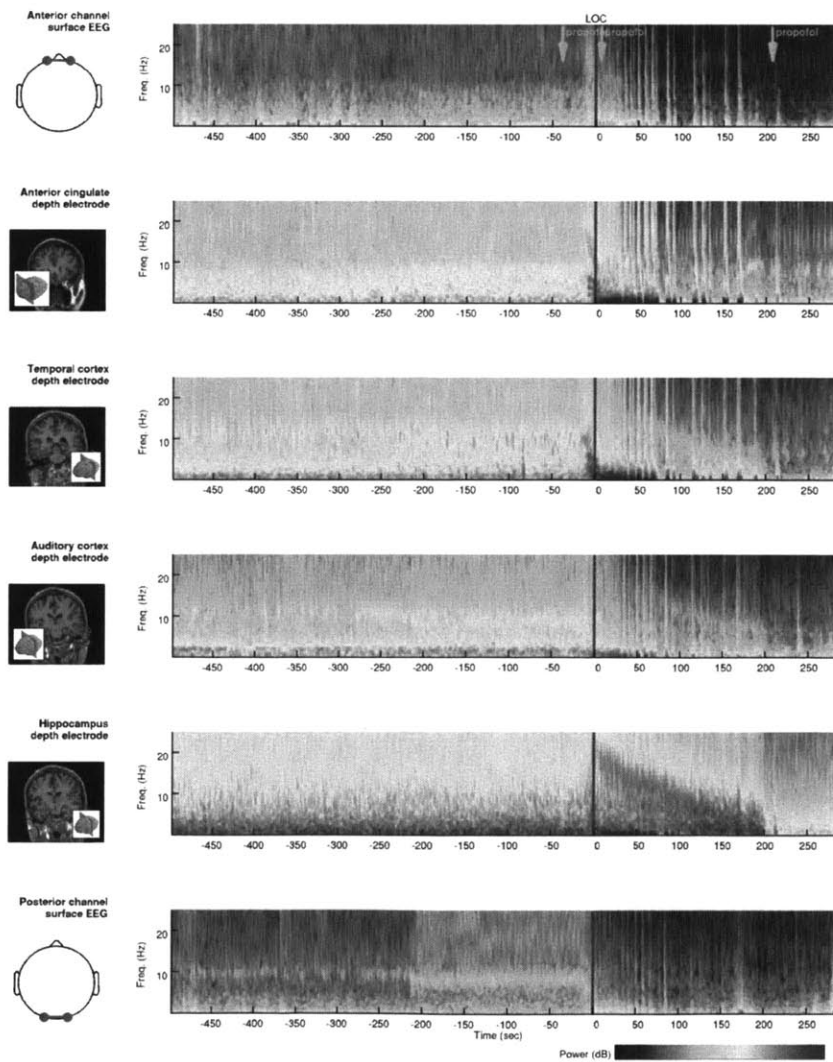


FIGURE S2. Exemplar spectrograms during induction of propofol anesthesia, patient 1.

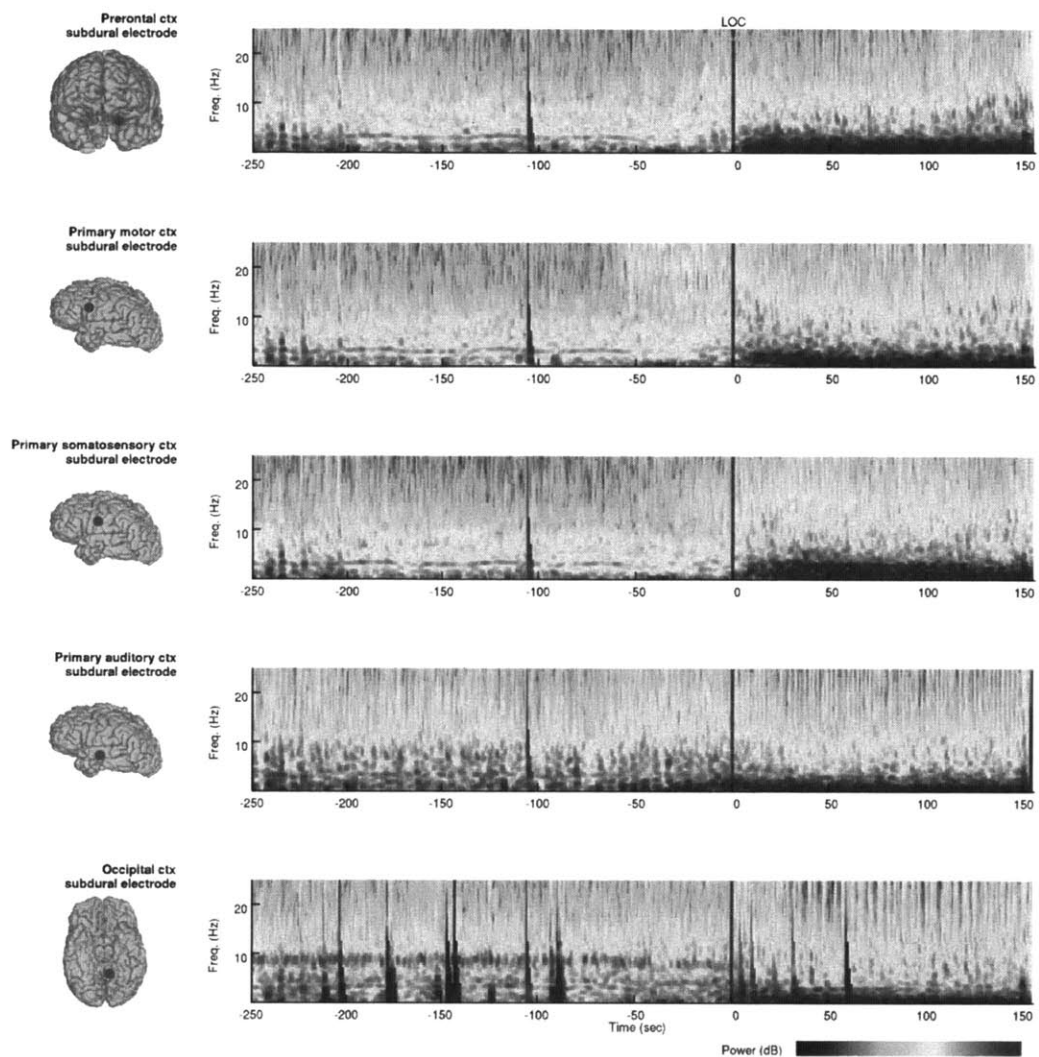


Figure S3. Exemplar spectrograms during induction of propofol anesthesia, patient 2.

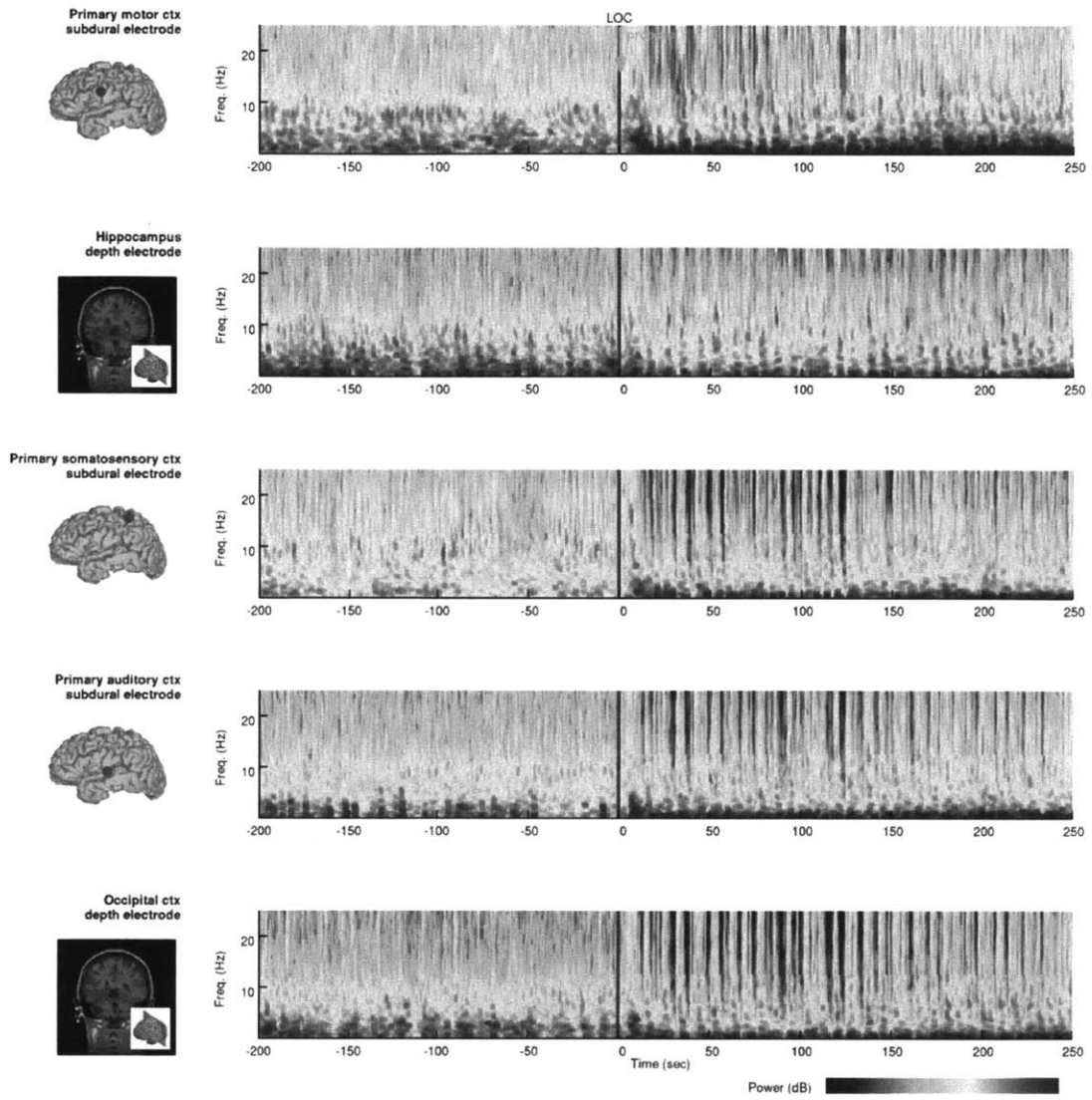


Figure S4. Exemplar spectrograms during induction of propofol anesthesia, patient 4.

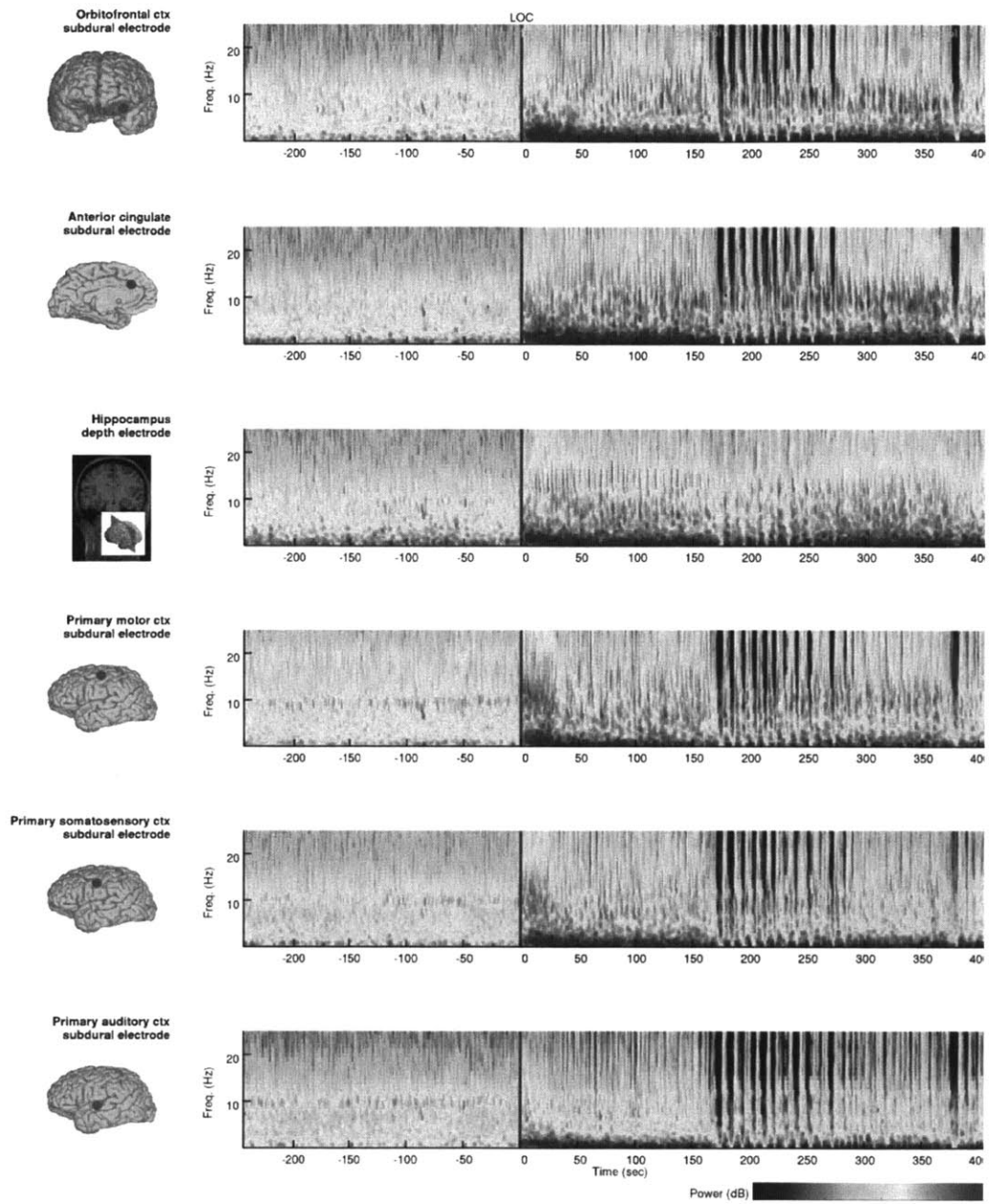


Figure S5. Exemplar spectrograms during induction of propofol anesthesia, patient 5.

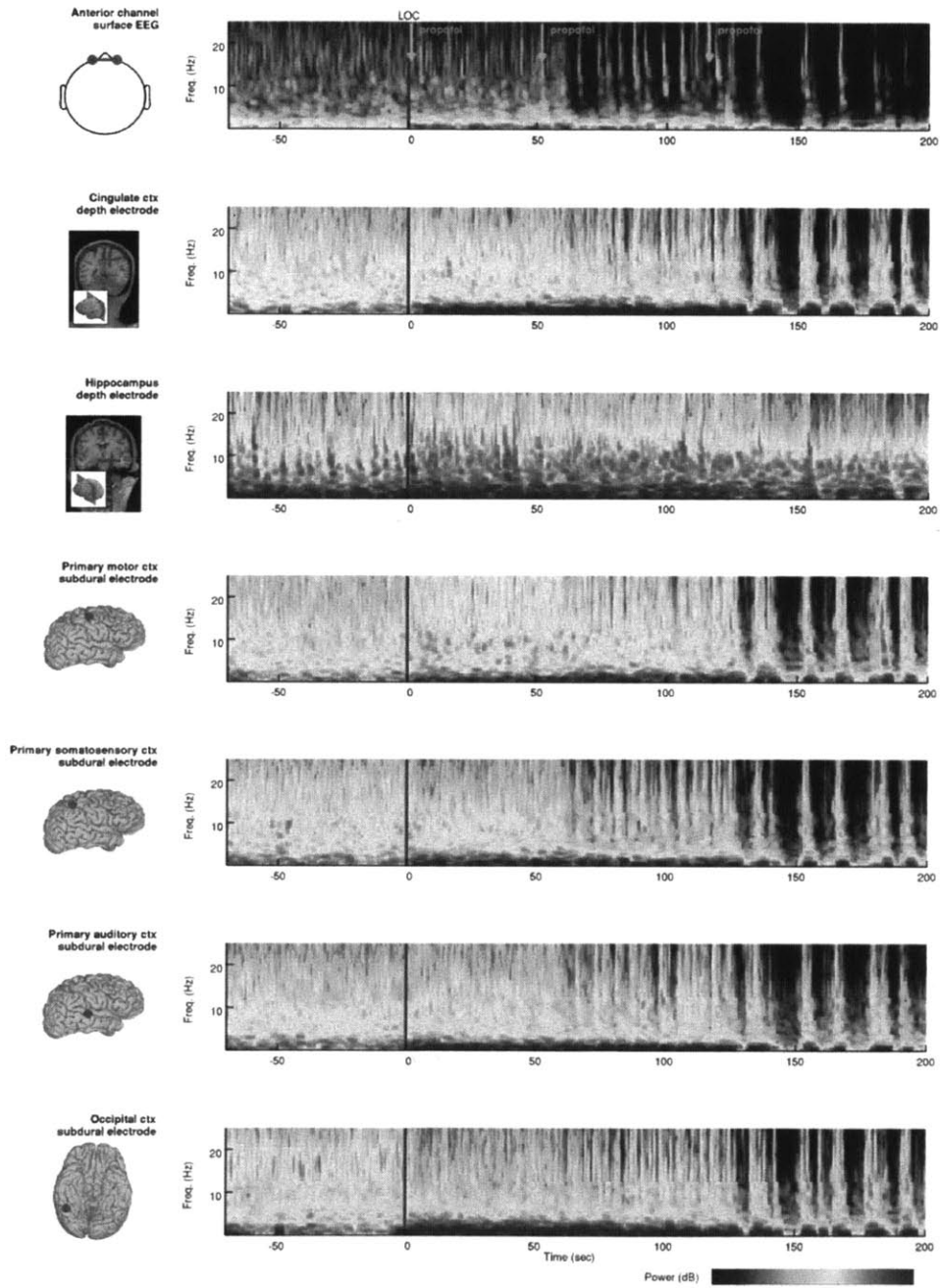


Figure S6. Exemplar spectrograms during induction of propofol anesthesia, patient 6.

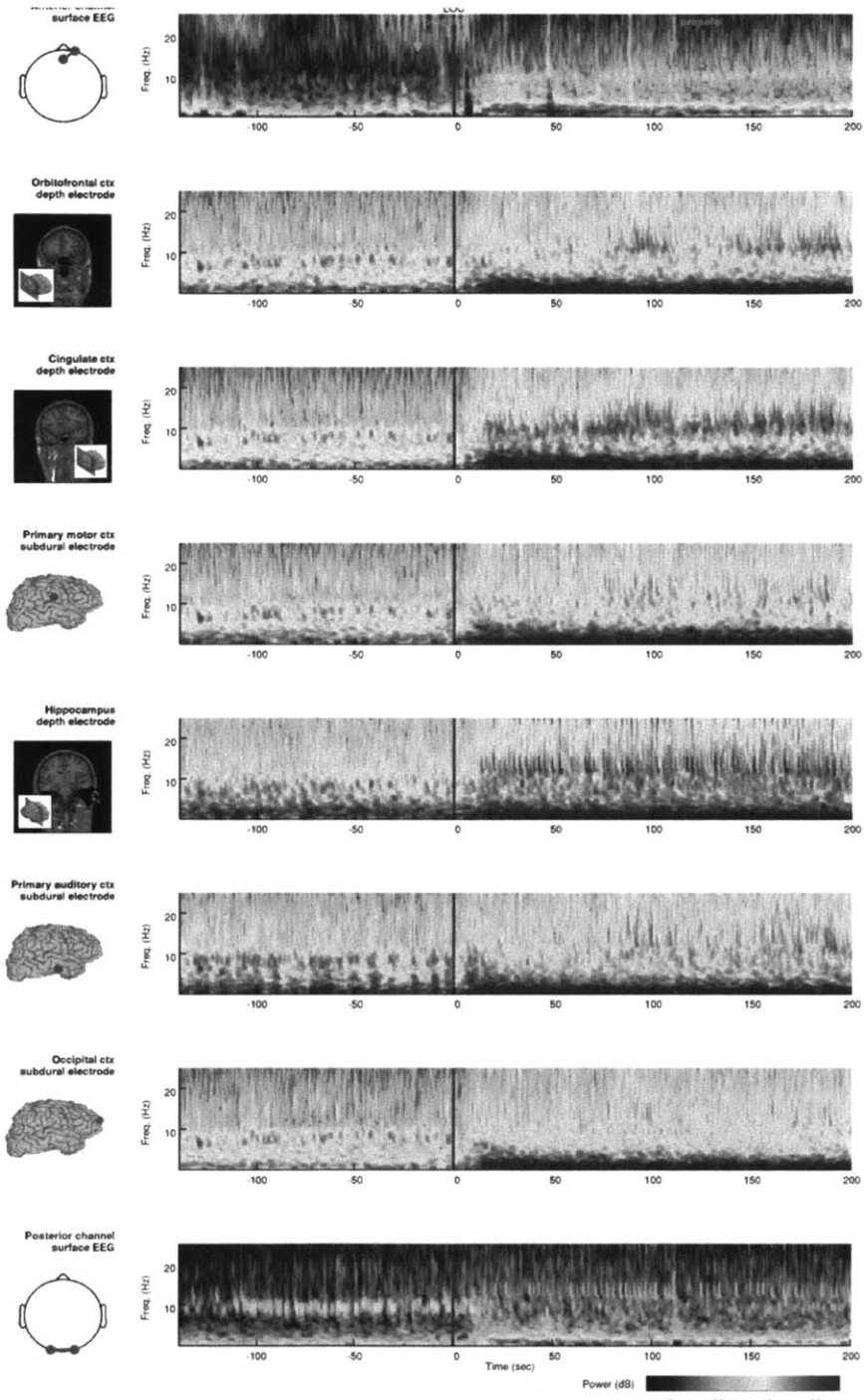


Figure S7. Exemplar spectrograms during induction of propofol anesthesia, patient 7.

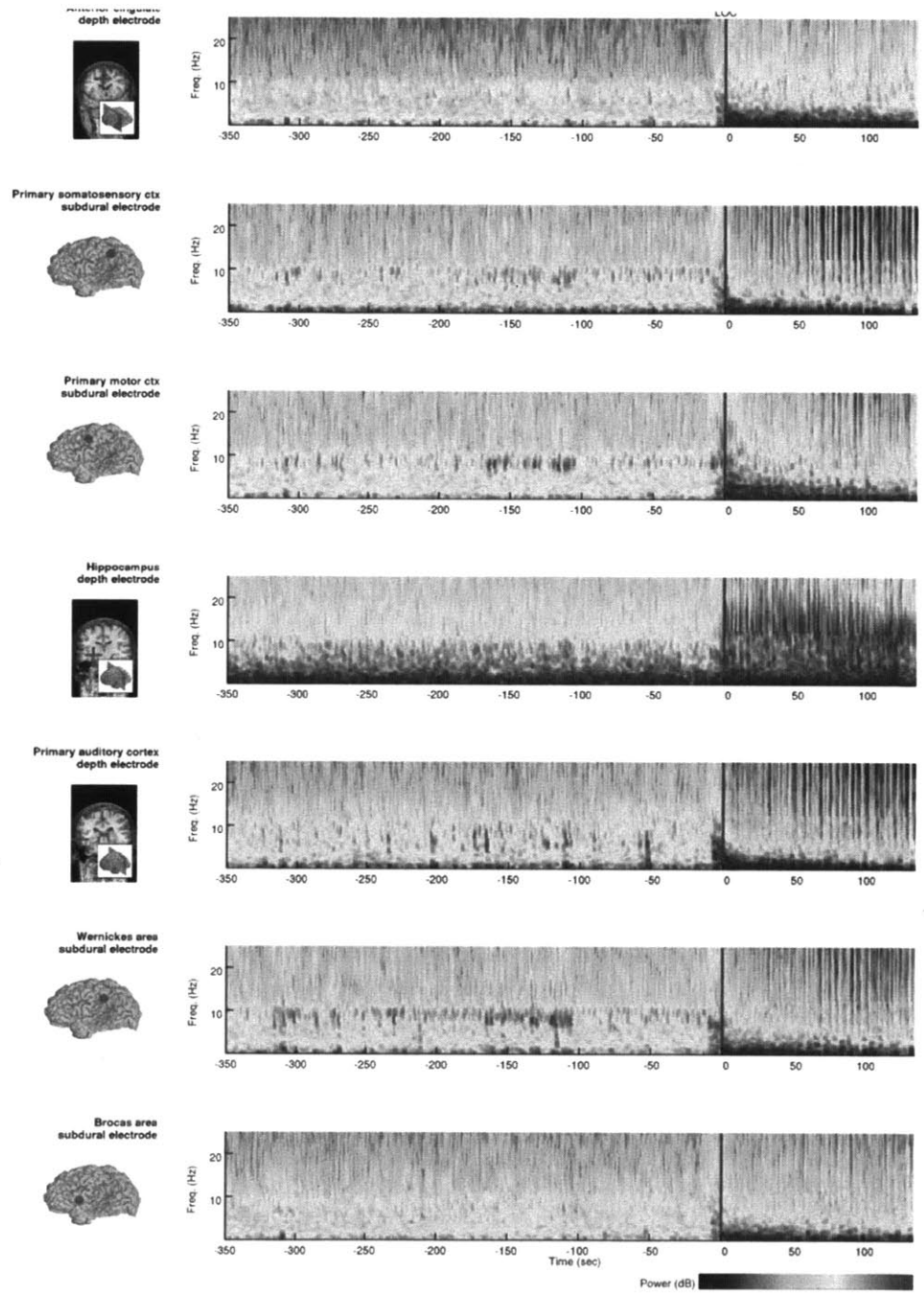


Figure S8. Exemplar spectrograms during induction of propofol anesthesia, patient 8.

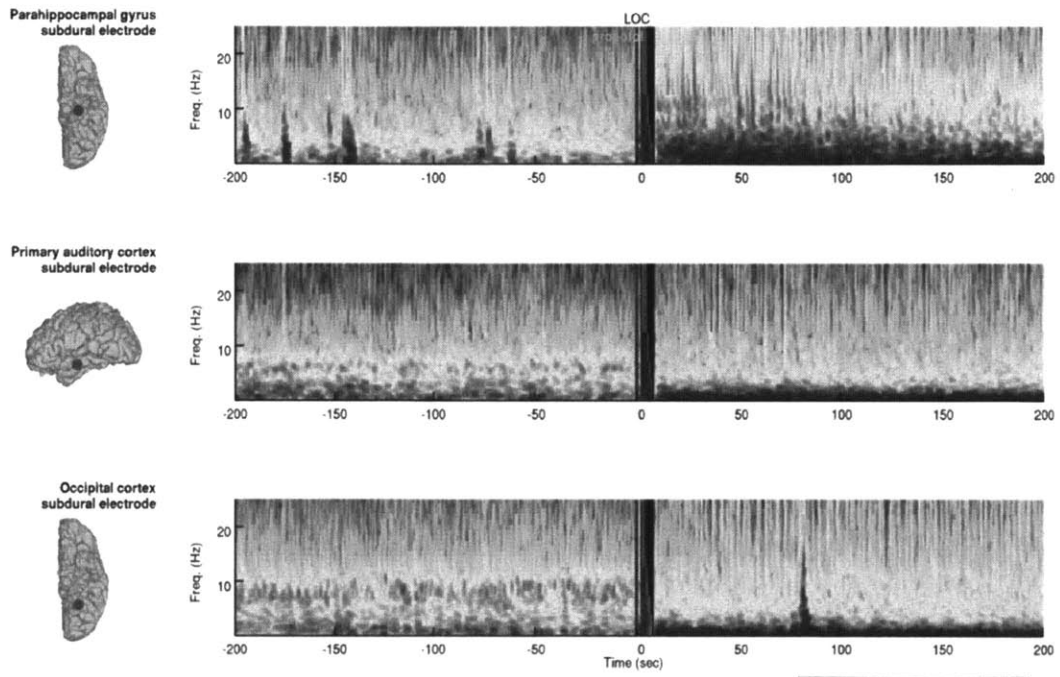


Figure S9. Exemplar spectrograms during induction of propofol anesthesia, patient 10. Half the surface rendering in the brain is shown due to artifacts in the MRI image for this patient.

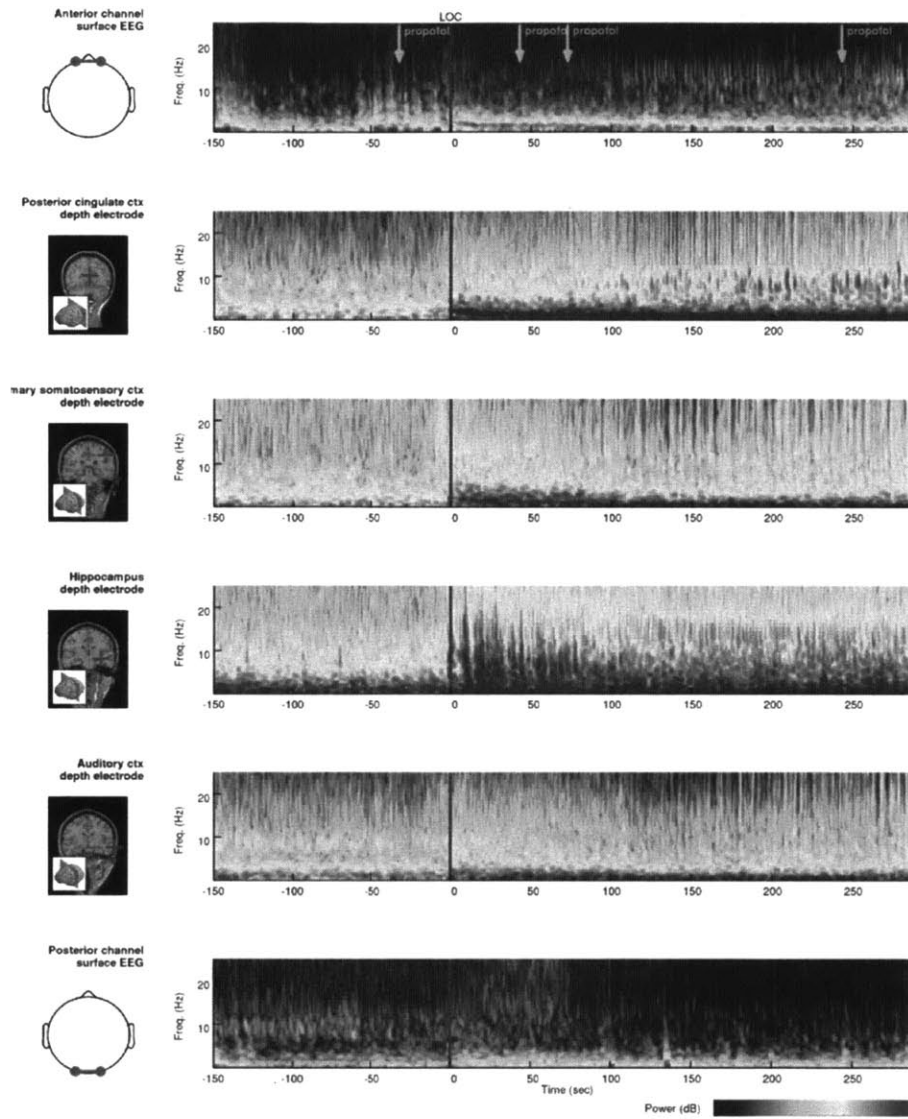


Figure S10. Exemplar spectrograms during induction of propofol anesthesia, patient 11.

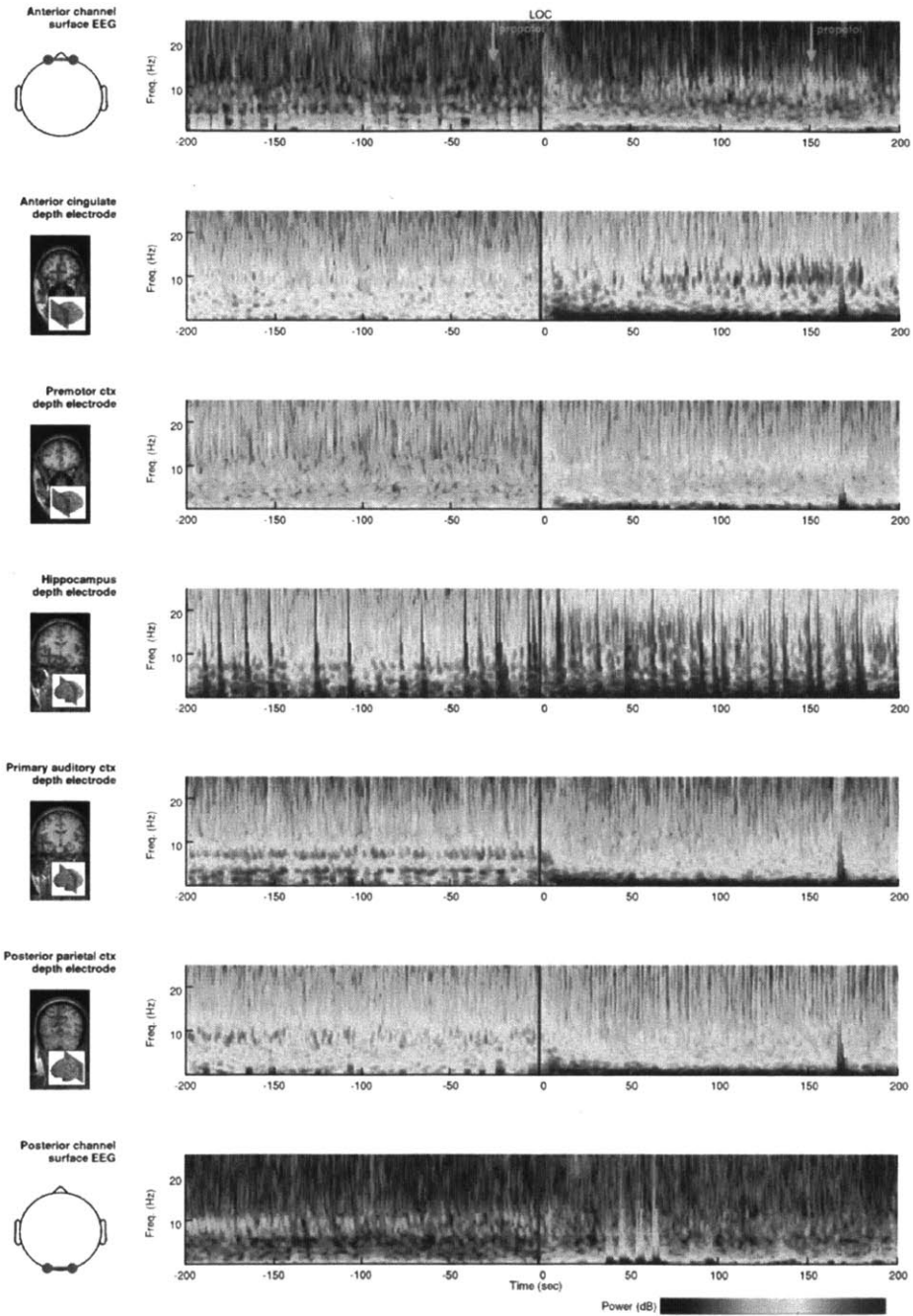


Figure S11. Exemplar spectrograms during induction of propofol anesthesia, patient 12.

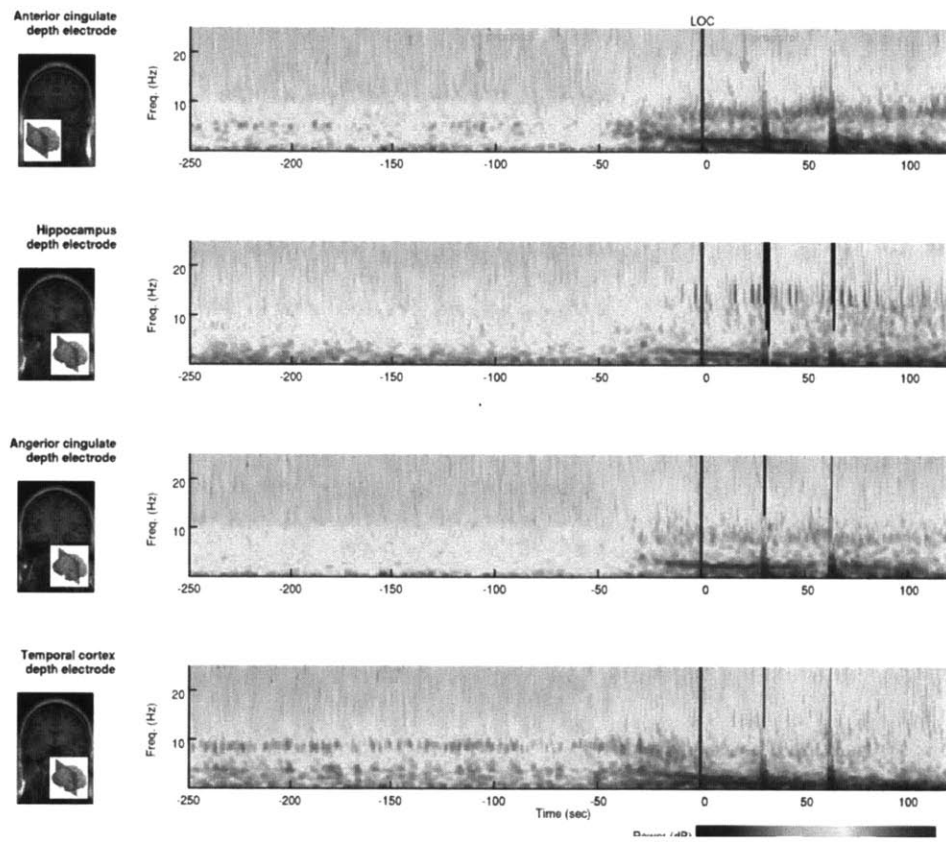


Figure S12. Exemplar spectrograms during induction of propofol anesthesia, patient 13.

Chapter 3: Global coherence analysis of intracranial recordings during induction of propofol general anesthesia

Abstract

It has been hypothesized that anesthetic drugs may induce unconsciousness by changing functional connectivity within and across brain regions. To test this hypothesis in humans, we examined recordings from a set of 14 patients who had been implanted with intracranial electrocorticography (ECoG) electrodes for the management of intractable epilepsy while they transitioned to unconsciousness with propofol. We used a frequency domain principal components analysis to identify coherent oscillatory modes in the data set across loss of consciousness.

Consistent with previous findings, we demonstrated an anterior shift of coherent activity in the alpha (8-12 Hz) frequency band. We also observed a medialization of coherent alpha activity toward the cingulate cortex and nearby recordings from white matter. This is consistent with the medialization of alpha power observed in recordings from single electrodes (Chapter 1).

Surprisingly, we observed a coherent, high-amplitude rhythm in the delta (1-3 Hz) to slow (0.1 to 1 Hz) frequency bands, also occurring in the medial frontal cortex and white matter recordings of those subjects with depth electrodes. This is in contrast with results from surface EEG and cortical ECoG recordings that demonstrate incoherent slow rhythms, and adds to evidence of distinct neocortical and subcortical effects of propofol.

Finally, we observed an abrupt cessation of coherent rhythms in the sensorimotor cortices at LOC. Coherent alpha and theta (4-7 Hz) networks that occurred over visual and auditory cortex during wakefulness, and the white matter in close proximity, ceased abruptly within seconds of unconsciousness with propofol bolus. Theta rhythms have been previously shown in human

temporal cortex, where they are thought to mediate long range functional connectivity as well as memory processes. Therefore, the disruption of these rhythms may lead to disruption of long-range connectivity as well as connectivity within the sensorimotor cortices, and may underlie some of the behavioral effects of propofol.

Introduction

General anesthetics do not globally suppress electrical activity in the brain; rather, they cause stereotyped features in the electroencephalogram (EEG) that are distinct from those in wakefulness, sleep, and coma (Brown, Lydic, & Schiff, 2010). Signatures of anesthesia in EEG have been described since the 1930s (Gibbs, F.A., Gibbs & Lennox, 1937). They have been shown in surface recordings (Gugino, 2001, John 2001, Feshchenko, 2004), high density EEG (Purdon et al 2012, Murphy et al 2011), and intracranial encephalography (ECoG) of the cortical surface (Breshears 2010, Lewis 2012). The spectral features of anesthesia include a high frequency rhythm that increases transiently near loss of consciousness (LOC), a widespread, high-amplitude asynchronous slow rhythm (Steriade, 1993), and an alpha frequency (8-12 Hz) rhythm that is distributed more frontally on the scalp than during wakefulness and increases to a higher frequency (~12-13.5 Hz). The *de novo* rhythms of anesthesia are concomitant with a reduction of EEG alpha power over the occipital cortex. During deep states of anesthesia, a pattern known as burst suppression may occur, with alternating periods of high amplitude electrical activity (bursts) and quiescence (suppressions). Signal amplitudes during burst suppression may be intermittently larger than those of wakefulness (Swank, 1949). Isoelectricity, while not necessary for unconsciousness, occurs during the deepest states of anesthesia.

While numerous EEG signatures of general anesthesia have been established, it is not well understood how anesthetic drugs suppress consciousness at a systems neuroscience level. The anesthetized brain remains highly electrically active; therefore, researchers have proposed that anesthetic drugs may suppress consciousness by modifying functional connectivity. Anesthetic drugs may impair information integration across brain regions (Tononi 2004, 2005, 2008, Baars 2005, Hudetz 2006, Alkire 2008, Mashour 2005). They may disrupt circuits that are specifically necessary for consciousness: circuits in the frontal, parietal, mediolateral, or cingulate cortices, the thalamus and its connections with cortex, and/or in the sensory networks that respond to stimuli (Antognini, 1997, Alkire 2008, Vogt 2005). Additionally, anesthetics may reduce the overall complexity of operations in the brain via stereotyped activity occurring across broad regions (Tononi 1998).

Previous studies have examined the network effects of general anesthesia by computing changes in connectivity across pairs of EEG surface electrodes. With increasing anesthetic depth, EEG coherence shifts toward anterior channels, increases between frontal and prefrontal channels, is disrupted across the hemispheres, and is disrupted across the anterior-posterior axis (Supp, 2011, Cimenser et al 2010, John 2001). These coherence changes are pronounced in the alpha frequency band, in which the increased frontal-prefrontal synchrony after LOC has been called “hypersynchrony” (Supp 2011).

Connectivity changes have also been assessed in numerous neuroimaging studies with PET and fMRI (reviewed in Hudetz, 2012). These studies demonstrate variable effects by dose, region, and anesthetic agent, with connectivity reduced in some conditions and increased in others. Such neuroimaging research must be interpreted in light of current uncertainty about the mapping between blood flow and electrical activity in anesthesia. Early anesthesia is characterized by

spectral changes including a large amplitude slow rhythm with oscillatory periods of several seconds, whose mapping with blood flow may be different from that in the waking state. There is evidence from slice recordings that subtypes of GABAergic neurons may affect vasoactive pathways directly (Hamel 04), and those subtypes are variably distributed across cortex and subcortical regions. Therefore, the vascular effects of GABAergic drugs like propofol may vary by brain region. Directly recording electrical activity is important to accurately measure those effects of anesthetic drugs on neuroelectric connectivity distinct from its vascular effects.

Human ECoG offers the opportunity to examine electrical activity recorded from human brain tissue with high temporal and spatial resolution. Recently, an analysis of a subset of the current ECoG data set (3 patients) assessed phase coherence in cortex between distant slow frequency (0.1-1Hz) rhythms which were recorded simultaneously with single unit activity (Lewis 2012). This work showed that slow phase relationships are incoherent across several centimeters of cortex, and established that the anesthetized state is characterized by disjoint neural firing and a fragmentation of cortical connectivity. Another analysis of human ECoG recordings with propofol, in a seed-based connectivity analysis of a cortical grid electrode array, suggested that the connectivity patterns of wakefulness were maintained in sensorimotor cortex after LOC. While demonstrating similar connectivity patterns before and after LOC, the latter study used time-domain cross correlation as the measure of coherence, which measures the relationship between the largest amplitude signal components. Such components be in the slow or even ultra-slow (<.1 Hz) bands in human recordings. Therefore, it is an open question how connectivity may change in other functionally relevant frequency bands that are active during wakefulness, and how it may change in sites outside of sensorimotor cortex.

We obtained neural recordings from 14 patients who were implanted with intracranial electrodes for the management of intractable epilepsy, while those patients were anesthetized with propofol in an operating room setting. The current study extends prior connectivity analysis of human ECoG with a recording of both depth and surface electrodes, and with anatomical localization in subcortical and cortical sites. The recordings in this study were sampled from sites including the neocortex (temporal, frontal, somatosensory, motor, auditory, parietal, and visual), hippocampus, subcortical white matter tracts, and cingulate cortex. We used a frequency domain principal components analysis technique (Cimenser 2011) to identify the dominant oscillatory modes before and after the induction of anesthesia. We identified several region specific changes in the dominant oscillatory modes before and after LOC. These changes may be related to the behavioral effects of propofol.

Materials and methods

Data collection. 14 patients were implanted with intracranial ECoG electrodes for monitoring of medically intractable epilepsy prior to surgical treatment. Electrodes included a combination of subdural strip and grid arrays resting on the cortical surface, linear depth arrays penetrating subcortically (all from *AdTech, Racine, WI*) and surface EEG electrodes in a subset of the standard 10-20 configuration (n=7 patients). Electrode type and placement were determined by each patient's clinician independently of the current study. Written informed consent was obtained in accordance with the local institutional review board. Clinical and electrode information are provided in Chapter 1, Table 1.

We recorded data during the explant surgery which occurred after 1-3 weeks of invasive monitoring at Massachusetts General Hospital (n=12) or Brigham and Women's Hospital (n=2). Signals were acquired at 2000 Hz, 500 Hz, or 250 Hz sampling rates with hardware amplifiers

(XLTEK, Natus Medical, San Carlos, CA) bandpassing between 0.3 Hz and the sampling rate, and were stored on a computer for offline processing. For offline storage, data were referenced to an inverted ECoG electrode facing the inner skull table, a linked earlobe electrode (A1-A2) or an electrode on the back of the neck (C2). In one patient, data were stored without subtraction of a reference signal (patient 11). We obtained a postoperative CT scan and a preoperative T1-weighted MRI for each patient.

Anesthesia. All patients received a bolus of propofol to induce general anesthesia. Drug doses over the recording period were selected by the surgical anesthesiologists and are reported in Figure S1.

Behavioral tasks. In order to precisely assess the timing of loss of consciousness and to identify changes in task-related signal features, we instructed patients to perform an auditory task as they transitioned to unconsciousness. Auditory recordings of neutral words (e.g., “ladder” or “chair”) or the patient's name were delivered at four second intervals with a jitter of 1 second randomized uniformly, and patients responded with a button click. Stimuli were delivered using stimulus presentation software (Presentation, *Neurobehavioral Systems, Inc., Albany, CA*, or EPrime, *Psychology Software Tools, Inc., Sharpsburg, PA*). 13 patients performed the behavioral task; one patient was excluded by his clinician's request for logistical reasons (patient 10).

Data pre-processing. Data were pre-processed using custom software written in MATLAB (*The MathWorks, Natick, MA*) and an open-source brain imaging package (Freesurfer, <http://surfer.nmr.mgh.harvard.edu/fswiki>). We created a rendering of each patient's cortical surface from his or her MRI volume using Freesurfer's *recon-all* processing stream. We computed group average surface renderings and average MRI volumes for the patient group

using the same processing stream. We obtained each patient's ECoG electrode coordinates by performing a maximum intensity projection of the postoperative CT, then we manually matched the maximum intensity points to ECoG labels. We computed corresponding coordinates within the MRI by coregistering each patient's CT with his or her MRI using automated routines in Freesurfer. We obtained anatomical labels separately for the depth electrode arrays and the grid and strip electrode arrays as follows: for the depth arrays, we obtained anatomical labels from an automatic segmentation of the MRI in Freesurfer (Fischl et al., 2002). For the grid and strip arrays, we first mapped the electrode coordinates to their closest coordinates on the rendered cortical surface using a minimum energy algorithm (Dijkstra, 2011). We then obtained anatomical labels for the mapped grid and strip coordinates from an automated cortical parcellation in Freesurfer (Fischl et al., 2004). We verified each anatomical label by visual inspection of the MRI image.

Data exclusion. Electrodes predominated by artifacts (saturated or absent signal) were excluded. Shorter segments of data were excluded by visual inspection using the same criteria. Individual electrodes and shorter segments of data were excluded for epileptiform discharges. 14 channels were excluded for the appearance of dysplasia in the MRI. Data from two additional patients were collected during the same time period and were excluded from the current study on the because of of generalized or multifocal epileptiform discharges that could confound an assessment of coherent activity (all channels having epileptiform discharges in one patient, and 78/80 channels in the other patient). EEG data were recorded from 7 patients; we analyzed recordings from patients with at least six channels to ensure sufficient spatial coverage (n=4).

Data analysis.

Montaging. Previous studies have shown that reference noise may contaminate estimates of coherence predominantly at 15 Hz and above. Therefore, we computed a bipolar montage of the data set prior to analysis to reduce common reference artifacts. We selected a nearest neighbor montage in which no two bipolar channels shared a parent channel. This montage preserved linear independence among channels for the subsequent coherence analysis. We also repeated the all of the analyses in this work using a referential montage as described in *Data Collection*, in order to assess low frequency coherence, as estimates of coherence <10 Hz are unlikely to be affected by common reference noise.

We downsampled the referentially montaged and bipolar signals to 250 Hz using an anti-aliasing finite impulse response (FIR) filter then notch filtered the signals at 60 Hz and its harmonics. For display in Figures 4-16, we also bandpassed the signals between 0.3 Hz and 40 Hz using an FIR filter.

Epochs. We labeled loss of consciousness (LOC) as the period [-4 1] seconds surrounding the first auditory stimulus to which the patient did not respond. We identified burst and suppression periods using the amplitude threshold method described in (Lewis et al, in submission). We defined a pre-induction epoch that extended from the start of recording to the first propofol dose. We defined a post-induction epoch that extended from LOC to the first period of bursting or suppression, or the end of the recording, whichever was first.

Principal components analysis. We performed a global coherence analysis (Cimenser et al., 2011) to characterize the principal oscillatory modes in each patient's channel set. This is a principal components analysis in the frequency domain; it identifies the principal modes of oscillation over a set of signals at a frequency f . We performed this analysis separately for the

ECoG and EEG channel sets for each patient at frequencies 0.3-50 Hz. Using the toolbox Chronux (<http://www.chronux.org>) for multitaper spectral estimation, we estimated the cross spectral matrix for each set of ECoG or EEG channels at each frequency f . We used the following multitaper parameters: time-bandwidth product $TW = 2$, tapers $K = 3$, and window lengths T_f and spectral resolutions W_f that were chosen in a frequency specific manner (Supplementary Table 1). We computed the median of the real and imaginary parts of the cross-spectral matrix (Wong, 2011) over time windows spanning each epoch described above (pre-induction, post-induction, bursts, and suppressions). We also computed the median over shorter segments (3 window lengths T_f) to obtain a time varying estimate of the cross spectral matrix. Subsequently, we performed an eigenvalue decomposition of each median cross spectral matrix. The largest eigenvalue u_{i_max} corresponds to the dominant mode of oscillation at each frequency f . We multiplied the corresponding imaginary-valued eigenvector v_{i_max} by its complex conjugate to $v_{i_max}^*$ to obtain a real-valued vector of weights, w_{i_max} , summing to one. This vector of weights provides a set of channel coefficients proportional to each channel's contribution of spectral power to the dominant oscillatory mode at frequency f . We also computed the ratio of each eigenvalue u_i to the sum of eigenvalues. This ratio expresses the proportion of variance accounted for by the i th oscillatory mode, and for the dominant mode it is called the global coherence.

To examine how the spatial distribution of coherent activity changed over time, we computed a spatial center of mass for each oscillatory mode as the dot product of the channel weights w_i and the channel coordinates (r_i, a_i, s_i) in the MRI volume. For the bipolar channels in this analysis, spatial coordinates were derived as the midpoint of the two parent electrodes.

Modal projection analysis. We used a modal projection to characterize how the spectral power in the dominant oscillatory mode varied across states of consciousness. The modal projection is defined as in Wong, 2011. We estimated the spectra S in Chronux using the same parameters as above. In each condition, we aligned the modal projections for all patients to LOC and computed the median at each (t,f) across patients. Periods of data marked as burst or suppression epochs were not included in the median. We used a bootstrapping procedure to assess significance. For 200 replicates, we uniformly circle-shifted each patient's data within the spectral estimation windows t , then repeated the full coherence analysis on the shifted data to estimate a new median modal projection across patients. We resampled those replicates 500 times for improved resolution, to obtain a null distribution and compute the 95% confidence intervals at each (t,f) .

Results

We analyzed recordings from 14 patients. Electrode coverage is shown in Figure S1 (Chapter 1). Figure S1 shows the 75th percentile of spectral power, at each time t and frequency f , over the set of electrodes for each subject. The subjects demonstrated a variety of electrophysiologic features in their recordings related to electrode placement. Patients 8 and 11 had grid electrode coverage that included occipital cortex, and patient 2 had substantial temporal and auditory cortex coverage. Those patients demonstrated a high power alpha rhythm in wakefulness that is consistent with occipital and temporal/auditory alpha respectively. Patients 2, 3, 4, 5, 6, 7 and 10 had substantial electrode coverage in depth and frontal sites, and they showed an increase in alpha power after induction that is consistent with a general-anesthetic induced alpha rhythm at those sites. Patients 1, 8, 9, 10, and 13 had burst suppression for part or nearly all (patients 1 and 13) of the recording period. They demonstrated a waxing and waning of power in all frequency bands that is consistent with a burst suppression pattern.

Figures 1 and 2 show the results of a global coherence analysis in the set of patients computed using a bipolar montage. Figure 1 shows the median across the set of subjects during the pre-induction and post-induction epochs, with burst suppression periods excluded. Figure 2 shows the global coherence at each frequency and time, for each subject. At each frequency and time, the global coherence value is proportional to the spectral power in the dominant oscillatory mode. Patients similarly showed a variety of global coherence features that appear to be related to electrode placement. Nonetheless, as with the power dynamics shown in Figure S1, several invariant features emerged in the global coherence results. The patients with coverage in occipital and sensory cortices demonstrated global coherence in the alpha band prior to LOC. The patients with depth and frontal electrode coverage demonstrated coherent alpha and high alpha rhythms after LOC. The patients with burst suppression (1, 8, 9, 10, and 13) appeared to have high global coherence during the burst suppression period. Many patients (1-9) demonstrated an increase in delta and slow coherence after LOC. Patients 2,7, and 9 demonstrated a coherent ~15Hz rhythm during the first 100 seconds after LOC.

These changes in global coherence across the induction period are quantified in Figures S2 and S3 which shows the mean global coherence in each epoch, pre-induction and post-induction, for each patient at frequencies 0-20 Hz.

We identified spectral peaks in global coherence in each patient, in each condition, from the mean global coherence in each condition as shown in Figure S2 and S3. At each of those frequencies, for each patient, we computed the electrode weights (*Materials and methods*) and modal projection for the dominant oscillatory mode. These are shown in Figure 4 for an exemplar patient.

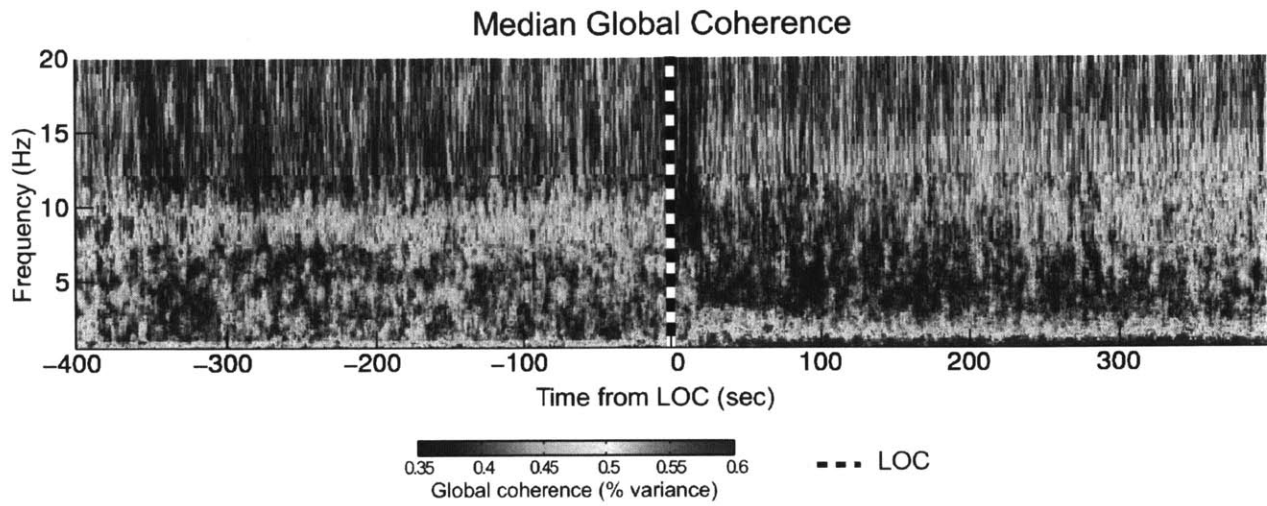


Figure 1. Median global coherence across the intracranial recordings for ten patients.

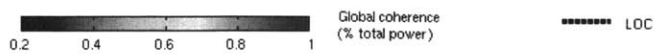
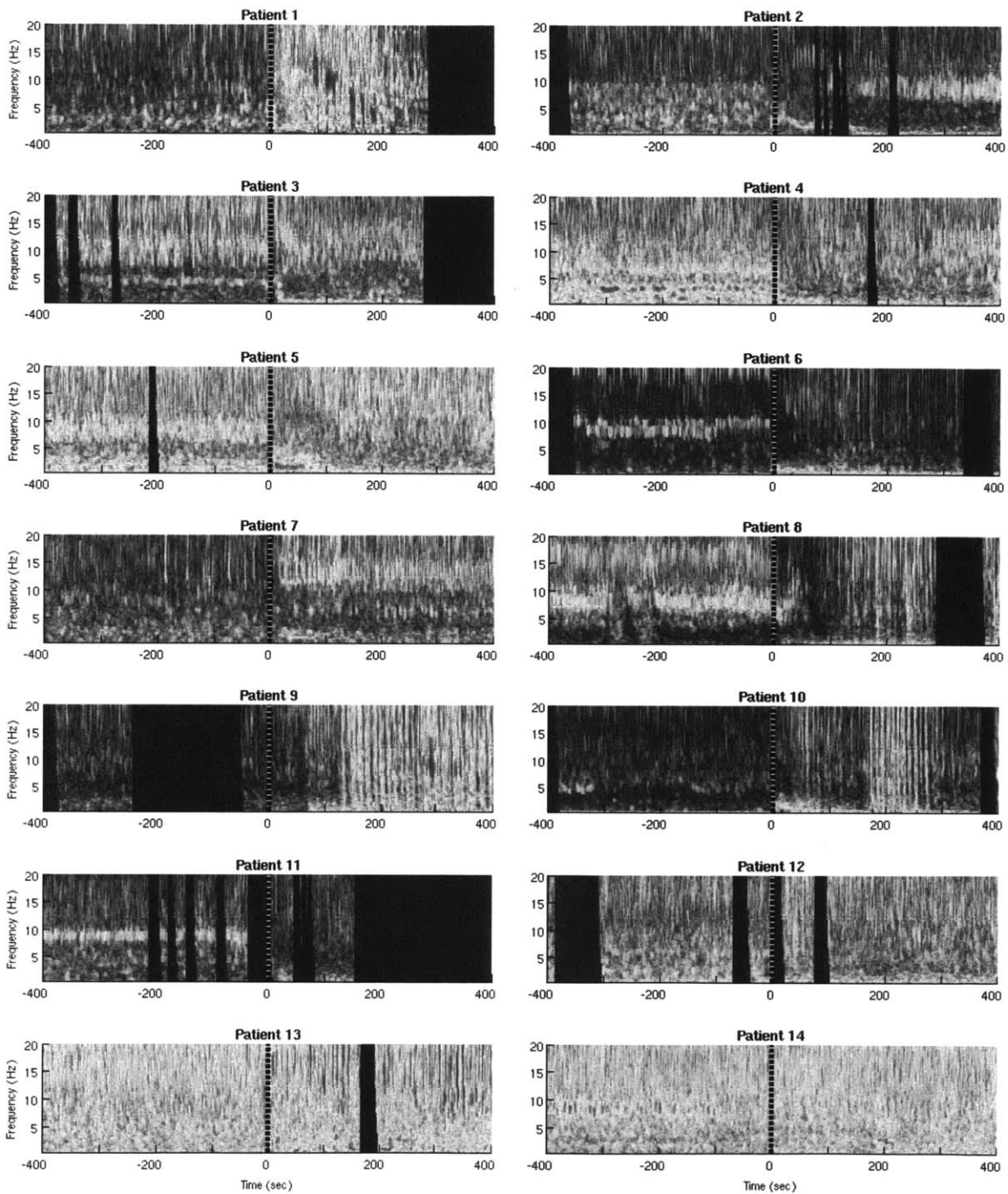


Figure 2. Global coherence across the recording period for each patient between 0-20Hz. LOC with propofol anesthesia is associated with changes in the predominant oscillatory modes from those in the waking state.

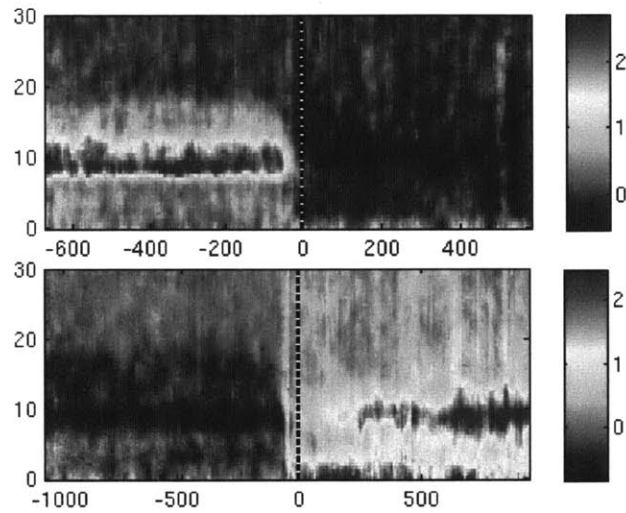
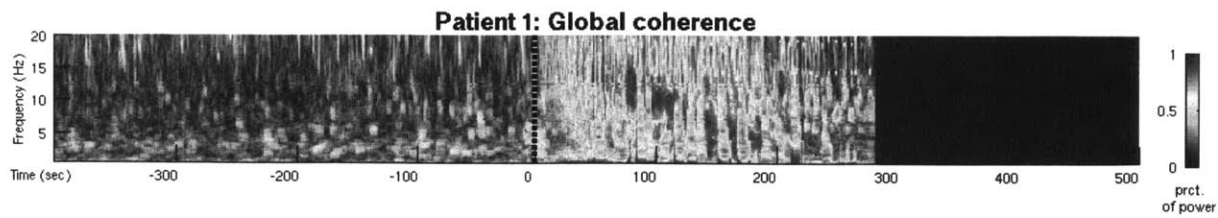
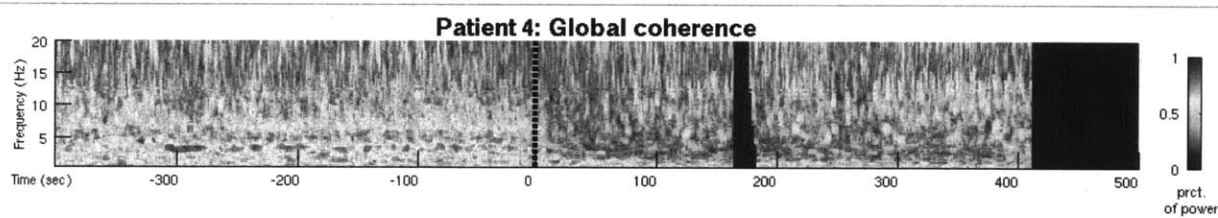
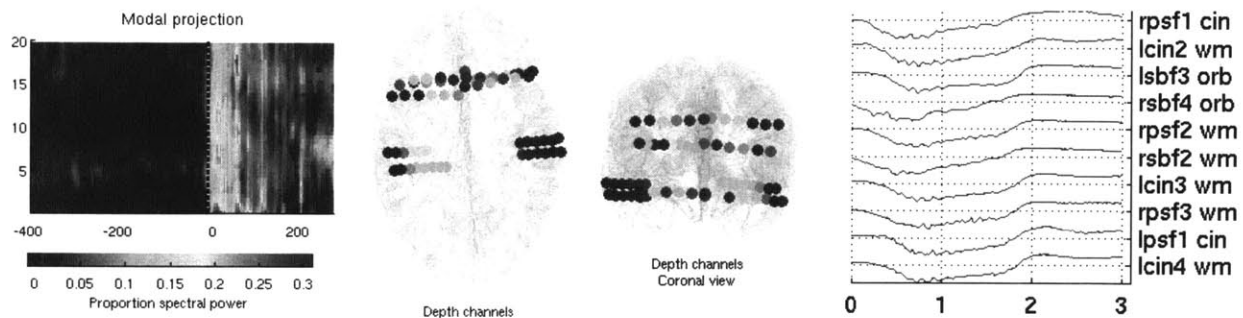


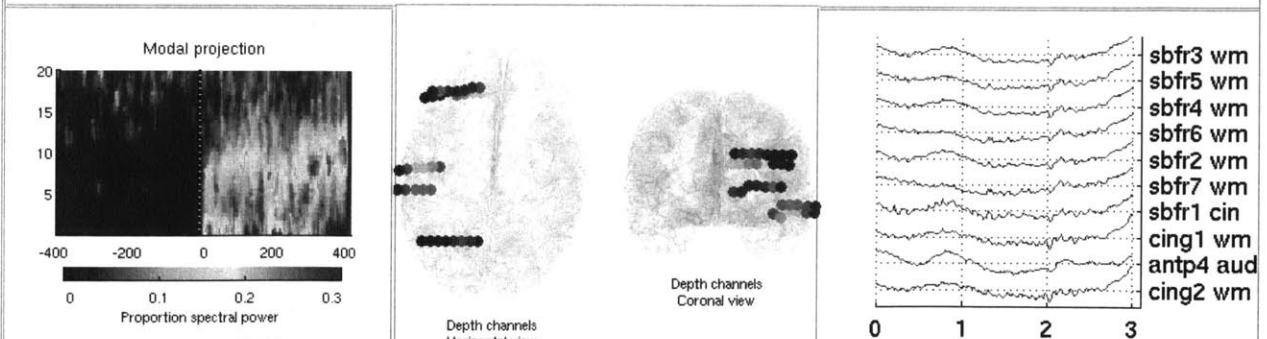
Figure 3. Normalized mean modal projection across subjects for the dominant oscillatory mode in the alpha band before induction (top panel) and after induction (bottom panel). The dominant mode was computed for patients with mean global coherence in the alpha band $>.4$ (Figures S2 and S3) in each epoch. Only those patients with global coherence above the threshold were included in the mean.



Principal mode at $f=0.3$, $t=49$



Principal mode at $f=1$, $t=31$



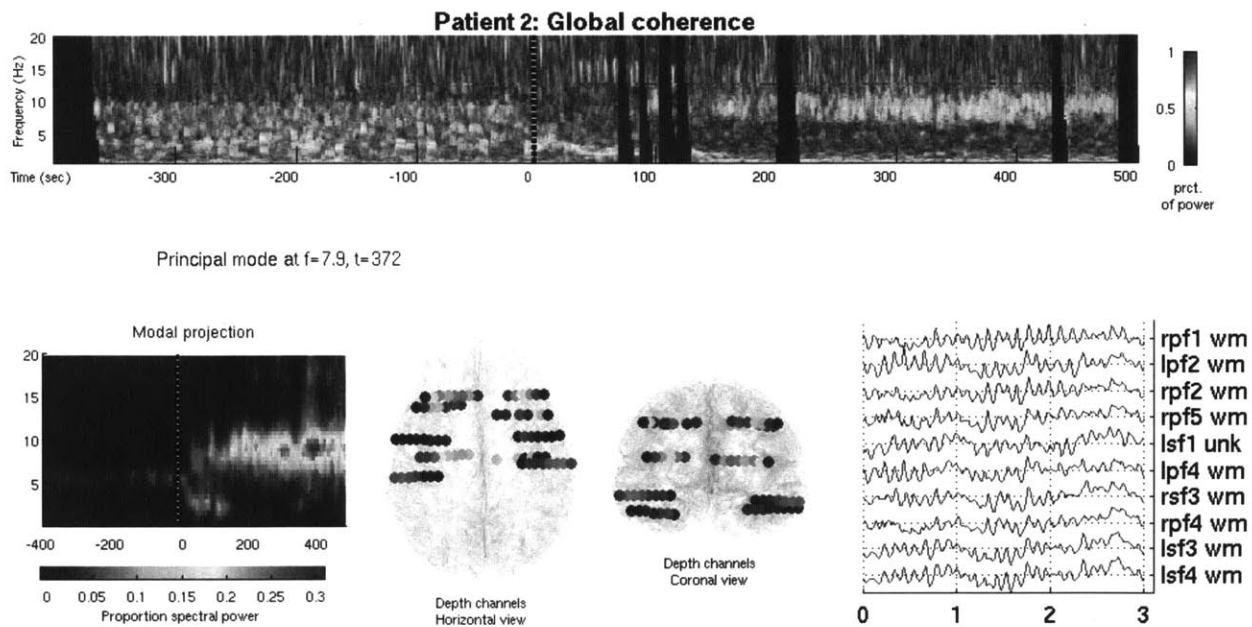
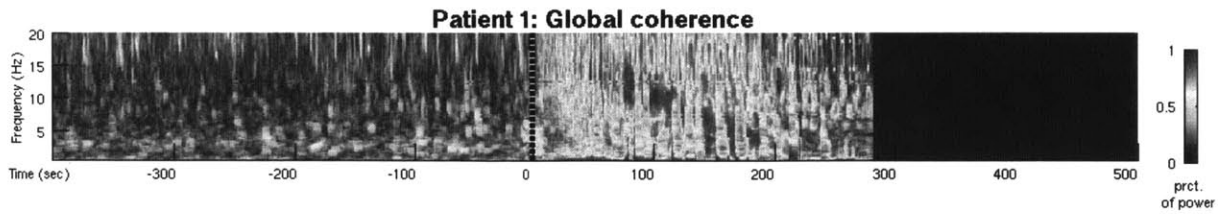
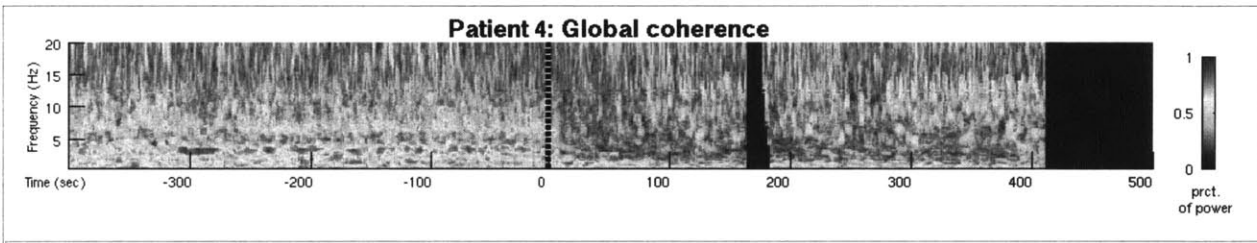
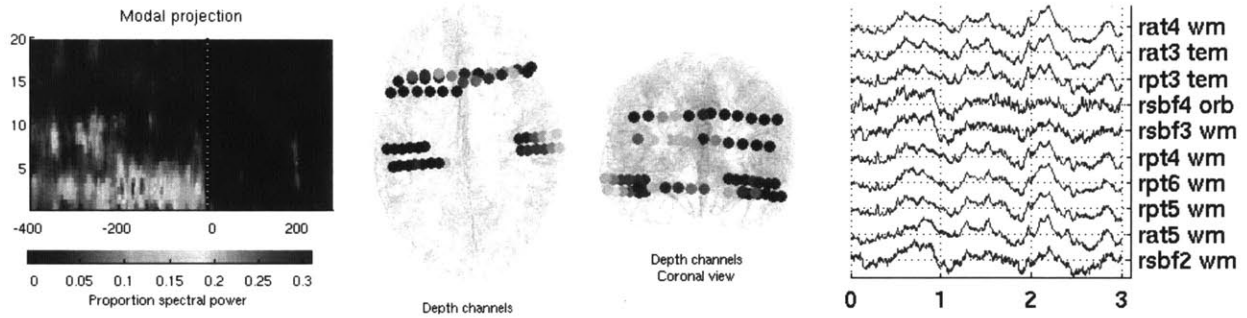


Figure 4. Coherent slow rhythms (top panel) in Patient 1, and coherent alpha rhythms (bottom panel) in Patient 2, emerge after LOC in medial channels. Coherent slow rhythms may occur as phase coupled with high frequency activity, can be observed in frontomedial white matter, cingulate cortex, and orbitofrontal cortex while being absent from the neocortex. Such rhythms occur in the same channels that are part of coherent alpha networks as depth of anesthesia increases.



Principal mode at $f=4.6$, $t=-131$



Principal mode at $f=6.6$, $t=-62$

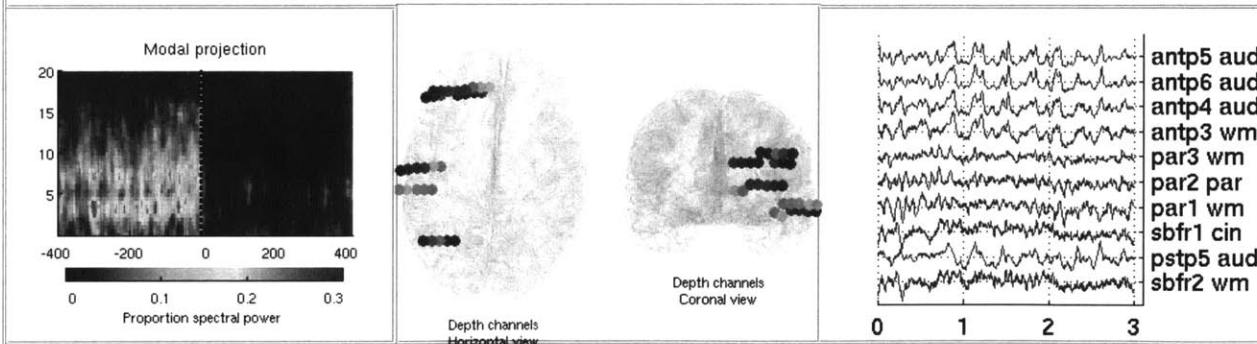


Figure 5. Theta rhythms are present in the temporal and auditory cortex prior to LOC and cease immediately at LOC.

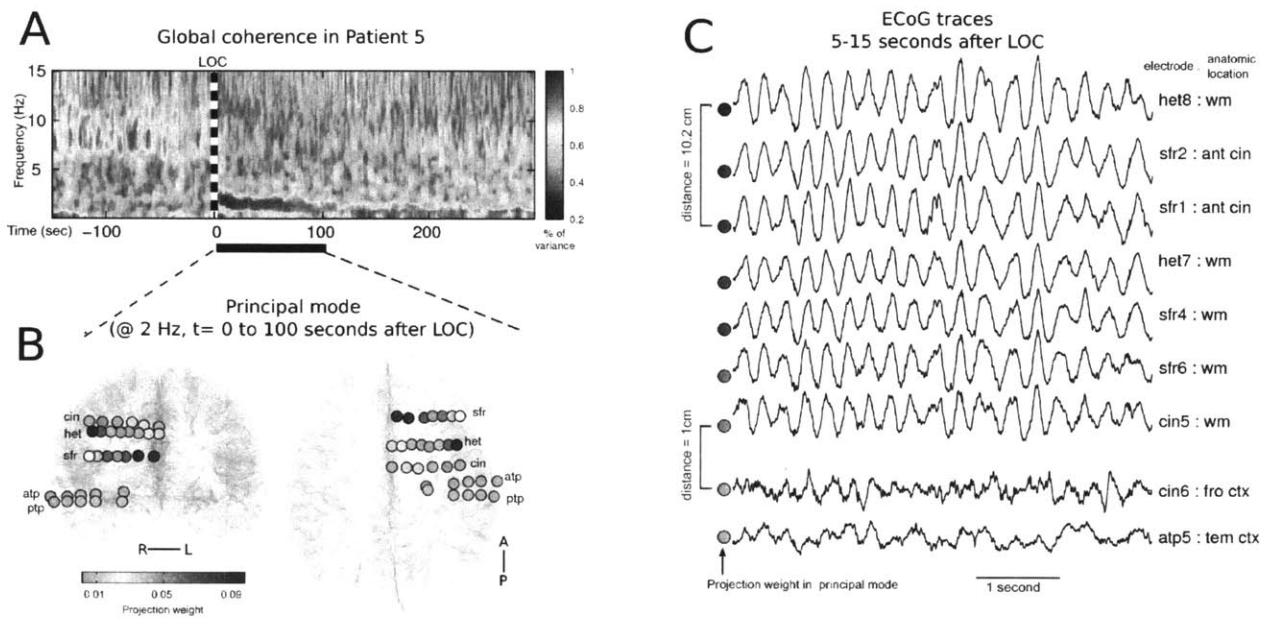


Figure 6. Global coherence zoomed-in plot for one patient showing high coherence in the delta to slow bands for 300 seconds after LOC. (B) shows the projection weights for electrodes in the dominant oscillatory mode at 2 Hz for a period of high global coherence after LOC. (C) shows example ECoG traces from electrodes in the dominant oscillatory mode.

Discussion

Using a combination of global coherence analysis and anatomical localization in ECoG electrodes, we analyzed spatiotemporal dynamics of the coherent oscillatory modes in the brain during the transition to unconsciousness with propofol.

Application of principal mode coherence analysis to ECoG recordings

A challenge of modern neuroscience is how to extract relevant structure from large sets of multielectrode recordings. The current dataset was collected during semi-natural conditions, while the patients performed an auditory task in a noisy operating room setting in an interrupted

manner. Moreover, the patients differed in recording sites, epileptic foci, drug doses and adherence to task. The global coherence technique nonetheless extracted invariant features from the set of 14 subjects across the transition to unconsciousness with propofol.

Coherent subcortical delta to slow rhythm

In contrast with results observed in high density EEG (Purdon in submission, Cimenser 2011), the patients in this dataset having depth electrodes demonstrated increased global coherence in the delta to slow frequency bands immediately following LOC. The coherence occurred primarily in the white matter tracts, cingulate cortex, and orbitofrontal regions with neocortical sites excluded. This result suggests that a) there may be a subcortical mechanism for generating delta and slow rhythms during anesthesia and b) that subcortical sites may be impaired in information transmission with neocortex in these frequency bands.

Medialization of alpha coherence

Coherence shifted from sensorimotor lateral networks in the temporal cortex and sensory networks in occipital cortex, to medial networks after LOC. This is consistent with a the medialization of alpha power reported in Chapter 1. This suggests the importance of subcortical generators in the rhythms of anesthesia, in addition to cortico-cortical mechanisms that may contribute to the regional effects of general anesthetics.

Bilateral incoherence in hippocampal rhythms

The previous chapter established that hippocampal power increases after loss of consciousness in the same data set, and in particular that the hippocampus remains active during the suppression periods of burst suppression. Here, we demonstrate a) hippocampal spindles in two patients, and

b) a coherent hippocampal alpha rhythm during suppressions. Both of these coherent rhythms appeared to be bilaterally incoherent. However, the electrode weights for these hippocampal rhythms suggested coherence in the same hemisphere, in temporal cortex and nearby white matter. A breakdown of hemispherical communication in the hippocampus may be related to the memory effects of propofol.

Disruption of the the alpha and theta rhythms of wakefulness: disrupted sensorimotor and long range connectivity

The coherent modes of wakefulness in the alpha and theta bands, in all patients where they were observed, ceased abruptly at LOC. These modes included recording sites within the sensorimotor cortices during wakefulness. An examination of the coherent oscillatory modes over time showed that coherent activity in the alpha and theta bands intermittently included recording sites in distant frontal regions and the hippocampus during the pre-induction period. The disruption of a coherent oscillatory mode in the alpha and theta bands may underlie the disruption of sensorimotor processing and long range transmission of sensorimotor information across brain regions with propofol.

Limitations

While the data were collected in epileptic patients, electrodes in the reported epileptic foci in each patient were removed to avoid the possibility that focal epilepsy may affect an analysis of connectivity. Furthermore, the dataset includes patients with numerous types of focal epilepsy, in many cases whose epilepsy achieved remission when those sites were resected. The coherence changes reported here may be confirmed in animal models.

We have observed a number of ECoG signatures of anesthesia that may be related to the effects of anesthetics in suppressing consciousness, by impairing functional network activity in a region specific manner.

References

- Andersen, P. (1968). *Physiological Basis of the Alpha Rhythm*. Plenum Pub Corp.
- Banks, M. I., White, J. A., & Pearce, R. A. (2000). Interactions between distinct GABA(A) circuits in hippocampus. *Neuron*, 25(2), 449-57.
- Behrens, T. E. J., Johansen-Berg, H., Woolrich, M. W., Smith, S. M., Wheeler-Kingshott, C. A. M., Boulby, P. A., Barker, G. J., et al. (2003). Non-invasive mapping of connections between human thalamus and cortex using diffusion imaging. *Nature neuroscience*, 6(7), 750-7. doi:10.1038/nn1075
- Breshears, J. D., Roland, J. L., Sharma, M., Gaona, C. M., Freudenburg, Z. V., Tempelhoff, R., Avidan, M. S., et al. (2010). Stable and dynamic cortical electrophysiology of induction and emergence with propofol anesthesia. *Proceedings of the National Academy of Sciences of the United States of America*, 107(49), 21170-5. doi:10.1073/pnas.1011949107
- Brown, E. N., Lydic, R., & Schiff, N. D. (2010). I 2638.
- Ching, S., Cimenser, A., Purdon, P. L., Brown, E. N., & Kopell, N. J. (2010). Thalamocortical model for a propofol-induced alpha-rhythm associated with loss of consciousness. *Proceedings of the National Academy of Sciences of the United States of America*, 107(52), 22665-70. doi:10.1073/pnas.1017069108
- Cimenser, A., Purdon, P. L., Pierce, E. T., Walsh, J. L., Salazar-Gomez, A. F., Harrell, P. G., Tavares-Stoeckel, C., et al. (2011). Tracking brain states under general anesthesia by using global coherence analysis. *Proceedings of the National Academy of Sciences of the United States of America*, 108(21), 8832-7. doi:10.1073/pnas.1017041108
- Feshchenko, V. A., Veselis, R. A., & Reinsel, R. A. (2004). Propofol-induced alpha rhythm. *Neuropsychobiology*, 50(3), 257-66. doi:10.1159/000079981
- Fox, J. ., & Jefferys, J. G. . (1998). Frequency and synchrony of tetanically-induced, gamma-frequency population discharges in the rat hippocampal slice: the effect of diazepam and propofol. *Neuroscience Letters*, 257(2), 101-104. ELSEVIER SCI IRELAND LTD. doi:10.1016/S0304-3940(98)00812-X
- Freund, T. F., & Antal, M. (1988). GABA-containing neurons in the septum control inhibitory interneurons in the hippocampus. *Nature*, 336(6195), 170-3. doi:10.1038/336170a0
- Gibbs, F.A., Gibbs, E. L., & Lennox, W. G. (1937). EFFECT ON THE ELECTRO-ENCEPHALOGRAM OF CERTAIN DRUGS WHICH INFLUENCE NERVOUS ACTIVITY. *Archives of Internal Medicine*, 60(1), 154-166. doi:10.1001/archinte.1937.00180010159012
- Hughes, S. W., & Crunelli, V. (2005). Thalamic mechanisms of EEG alpha rhythms and their pathological implications. *The Neuroscientist*: a review journal bringing neurobiology, neurology and psychiatry, 11(4), 357-72. doi:10.1177/1073858405277450
- Kuhlman, W. N. (1978). Functional topography of the human mu rhythm. *Electroencephalography and Clinical Neurophysiology*, 44(1), 83-93. doi:10.1016/0013-4694(78)90107-4
- Lehtelä, L., Salmelin, R., & Hari, R. (1997). Evidence for reactive magnetic 10-Hz rhythm in the

human auditory cortex. *Neuroscience letters*, 222(2), 111-4.

- Liu, W. H. D., Thorp, T. A. S., Graham, S. G., & Aitkenhead, A. R. (1991). Incidence of awareness with recall during general anaesthesia. *Anaesthesia*, 46(6), 435-437. doi:10.1111/j.1365-2044.1991.tb11677.x
- Lopes da Silva, F. ., Vos, J. ., Mooibroek, J., & van Rotterdam, A. (1980). Relative contributions of intracortical and thalamo-cortical processes in the generation of alpha rhythms, revealed by partial coherence analysis. *Electroencephalography and Clinical Neurophysiology*, 50(5-6), 449-456. doi:10.1016/0013-4694(80)90011-5
- Moller, J., Cluitmans, P., Rasmussen, L., Houx, P., Rasmussen, H., Canet, J., Rabbitt, P., et al. (1998). Long-term postoperative cognitive dysfunction in the elderly: ISPOCD1 study. *The Lancet*, 351(9106), 857-861. doi:10.1016/S0140-6736(97)07382-0
- Mukamel, E. A., Pirodini, E., Babadi, B., Wong, K. F. K., Pierce, E. T., Harrell, G., Walsh, J. L., et al. (n.d.). A novel transition in brain state during general anesthesia. *In submission*.
- Niedermeyer E. (1997). Alpha rhythms as physiological and abnormal phenomena. *International Journal of Psychophysiology*, 26(1), 19. Elsevier. doi:http://dx.doi.org/10.1016/S0167-8760(97)00754-X
- Pfurtscheller, G., & Andrew, C. (1999). Event-Related changes of band power and coherence: methodology and interpretation. *Journal of clinical neurophysiology*: official publication of the American Electroencephalographic Society, 16(6), 512-9.
- Purdon, P. L., Pierce, E. T., Mukamel, Eran A. Prerau, M. J., Walsh, J. L., Wong, K. F. K., Salazar-Gomez, A. F., Harrell, P. G., et al. (2012). Electroencephalogram Signatures of Loss and Recovery of Consciousness During Propofol-Induced General Anesthesia. *In submission*.
- Tinker, J. H., Sharbrough, F. W., & Michenfelder, J. D. (1977). Anterior shift of the dominant EEG rhythm during anesthesia in the Java monkey: correlation with anesthetic potency. *Anesthesiology*, 46(4), 252-9.
- Tort, A. B. L., Komorowski, R., Eichenbaum, H., & Kopell, N. (2010). Measuring phase-amplitude coupling between neuronal oscillations of different frequencies. *Journal of neurophysiology*, 104(2), 1195-210. doi:10.1152/jn.00106.2010
- Young, G. B., Blume, W. T., Campbell, V. M., Demelo, J. D., Leung, L. S., McKeown, M. J., McLachlan, R. S., et al. (1994). Alpha, theta and alpha-theta coma: a clinical outcome study utilizing serial recordings. *Electroencephalography and clinical neurophysiology*, 91(2), 93-9.

Supplementary Figures

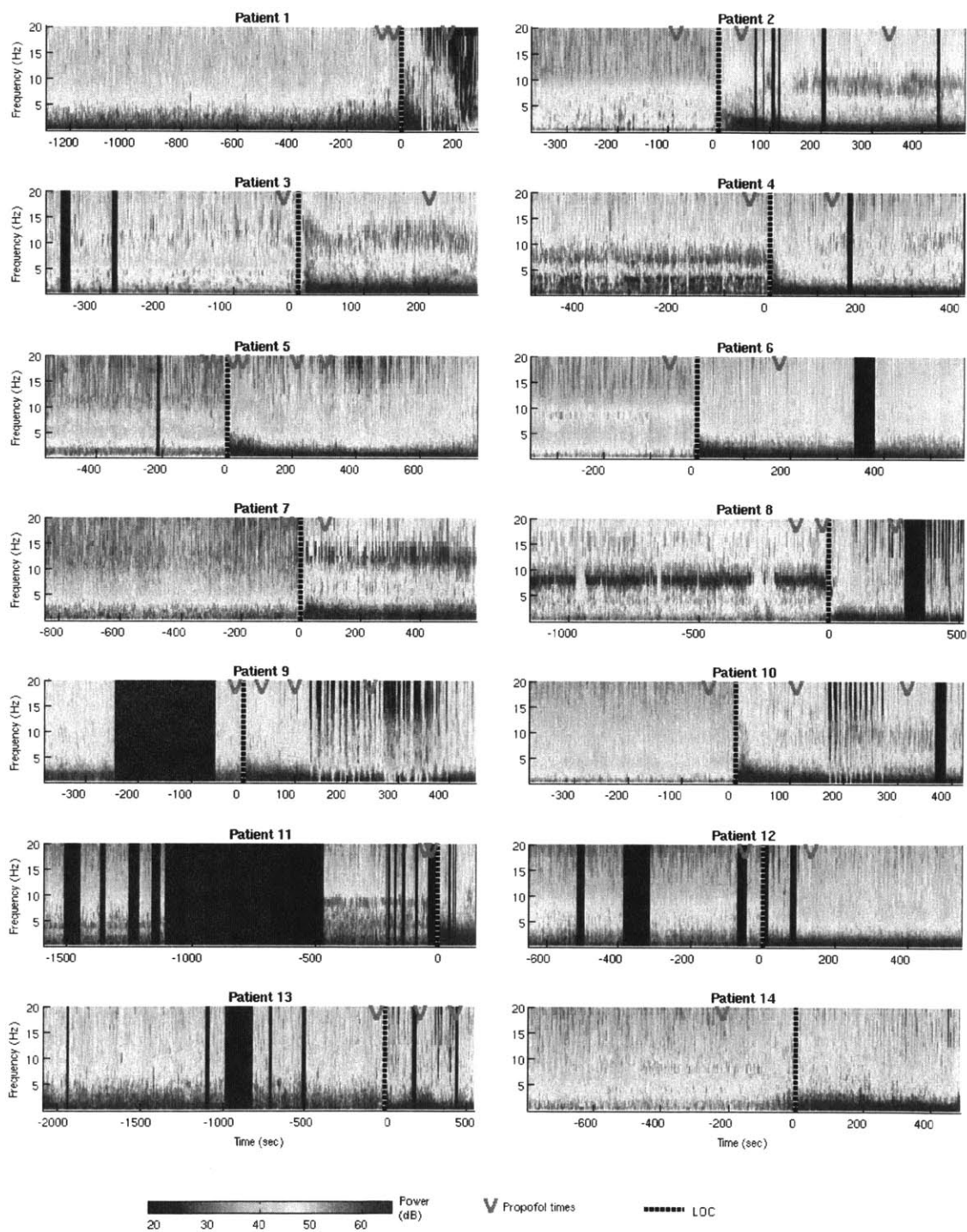


Figure S1. 75th percentile of spectral power between 0-20 Hz, over the recording period for each patient.

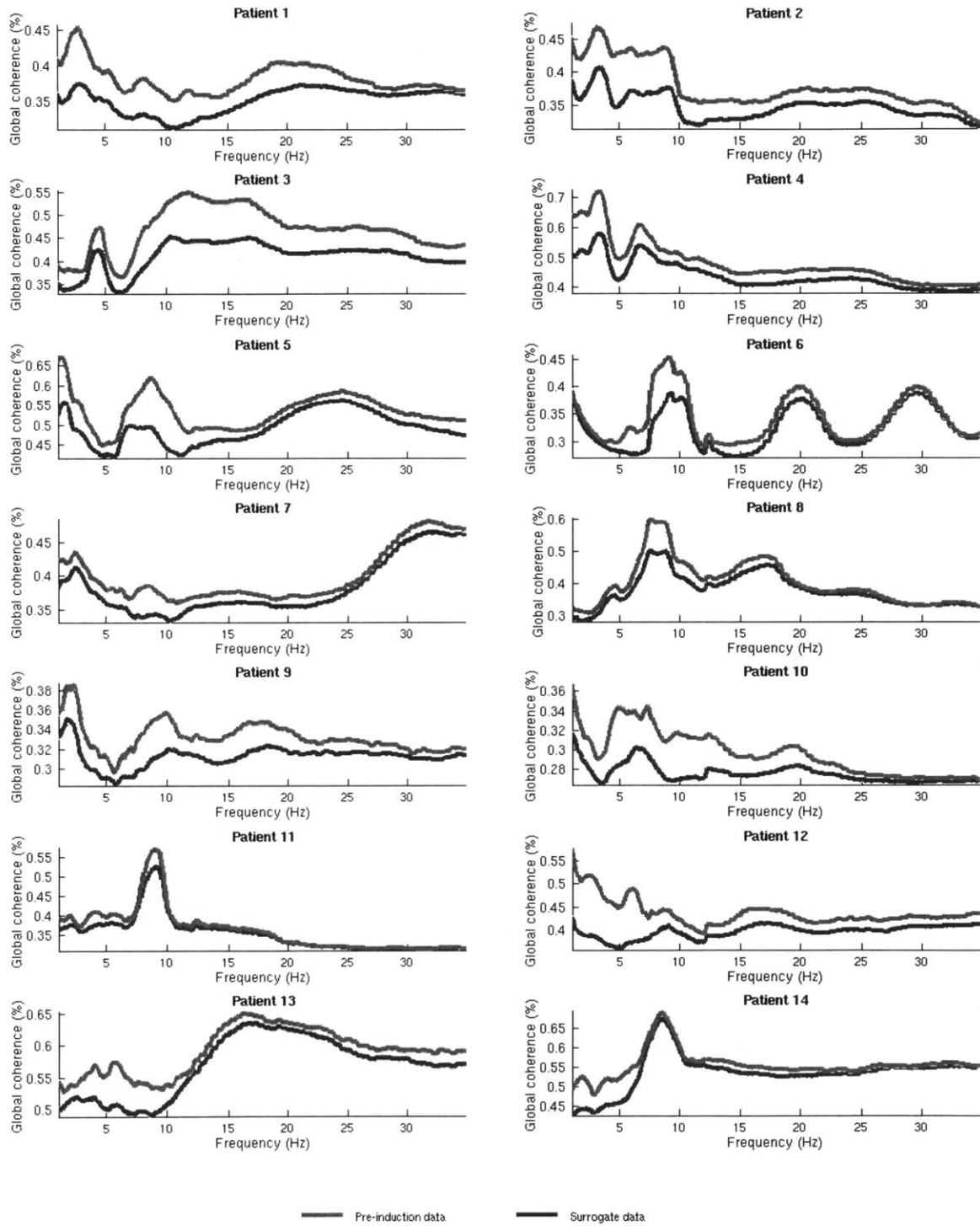


Figure S2. Mean global coherence by frequency before LOC for each patient. Shaded 5% confidence intervals are shown. Blue line shows mean results using surrogate data circle shifted within the cross spectral matrix estimation windows.

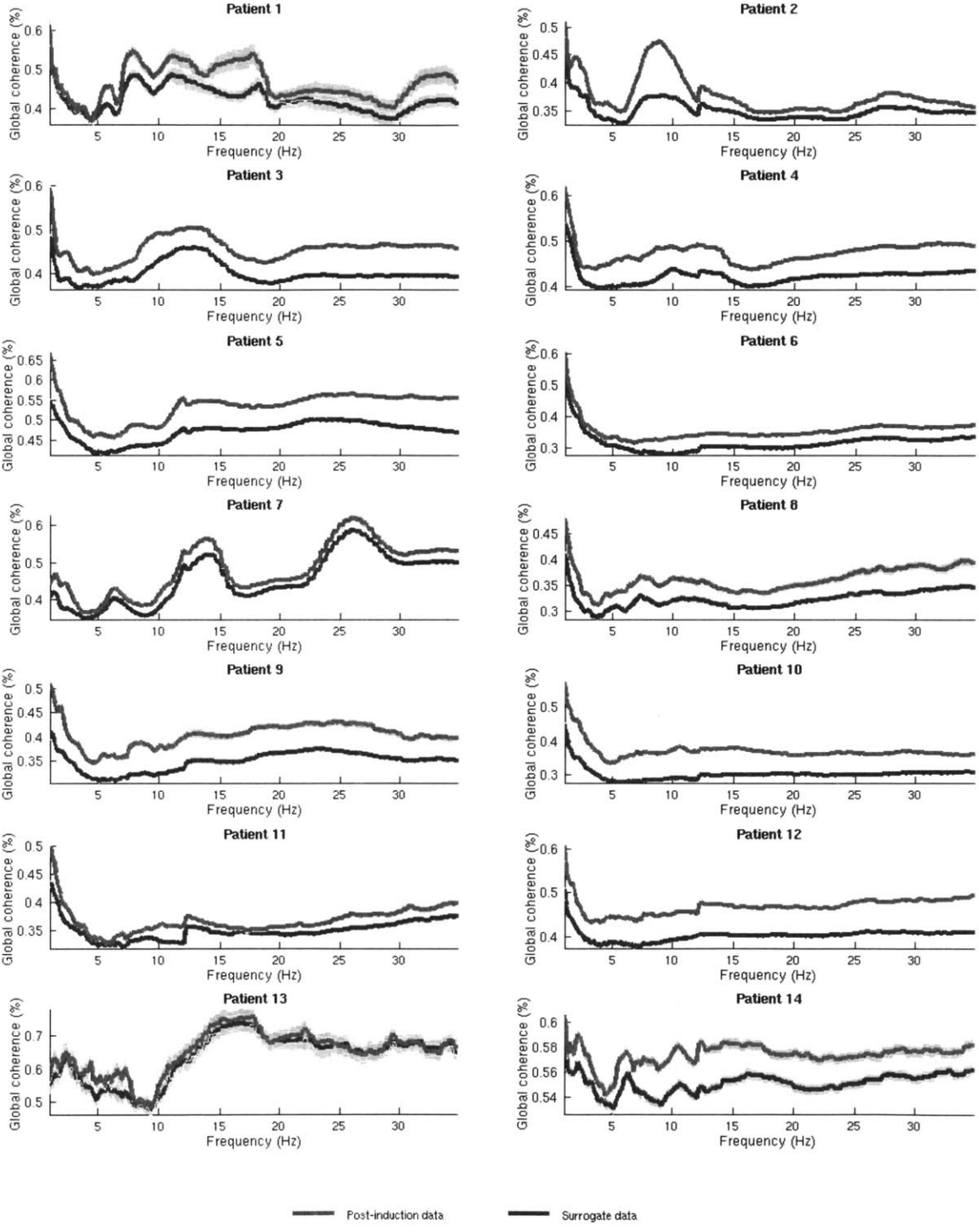


Figure S3. Mean global coherence by frequency after LOC for each patient during the post-induction epoch, exclusive of burst suppression intervals. Shaded 5% confidence intervals are shown. Blue line shows mean results using surrogate data circle shifted within the cross spectral matrix estimation windows. Patients 1 and 13 had <30 seconds of recording outside of burst suppression intervals.

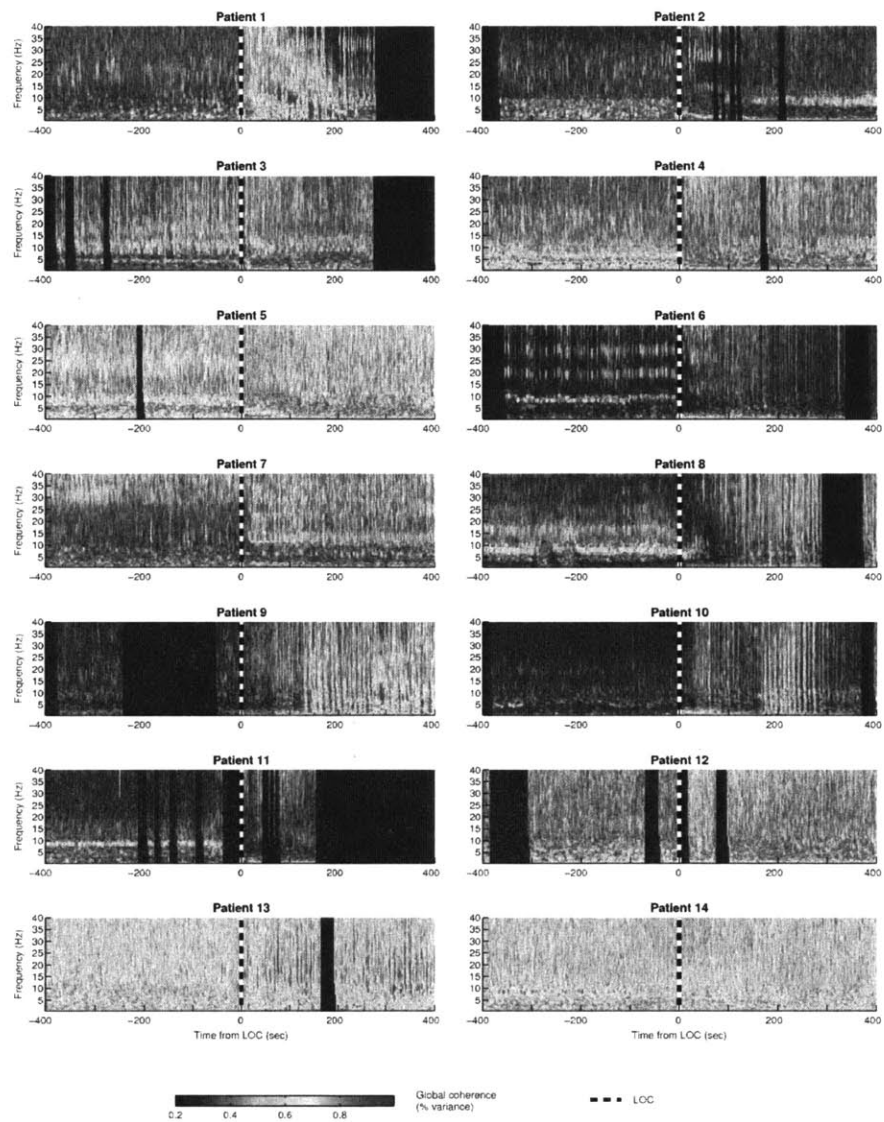


Figure S4. Global coherence in all subjects computed 0-40Hz with a bipolar montage.

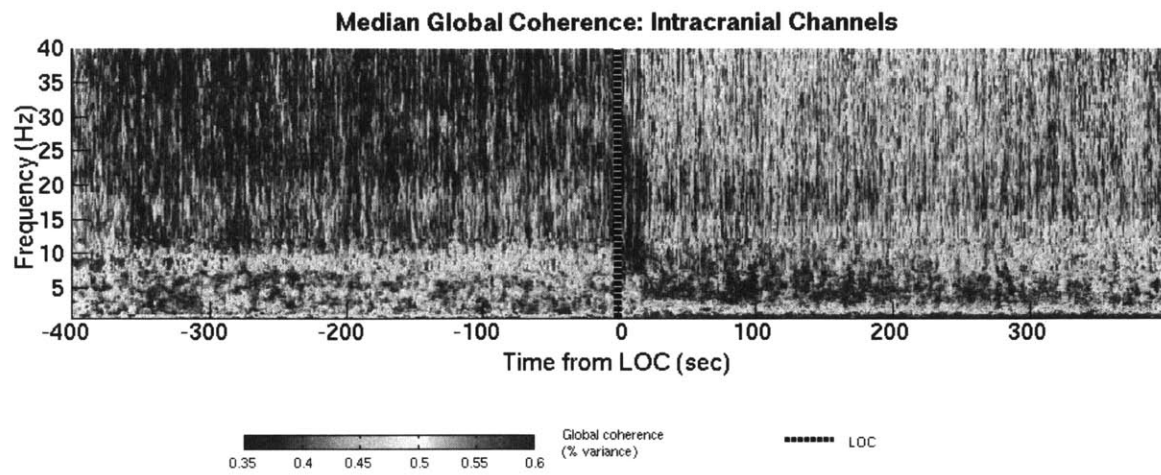


Figure S5. Median global coherence across all patients computed to 40Hz using a bipolar montage.